**NTNU – Trondheim**
Norwegian University of
Science and Technology

# Alternative methods to generate a first-order directional microphone

## Sebastia Vicenc Amengual Gari

# Preface

This thesis is presented in partial fulfilment of the requirements for the Degree of Telecommunication Engineering at the Polytechnic University of Catalonia. This thesis was completed at the Department of Electronics and Telecommunications of the Norwegian University of Science and Technology within the Erasmus Framework during the spring semester of 2014.

The project described in this document is part of a bigger project called SOUNDTRACK funded by the European Union's Seventh Framework Programme under the grant agreement num. 299620. SOUNDTRACK deals with redefining the aircraft noise monitoring systems to make them more reliable and independent from non-acoustic data. As a part of SOUNDTRACK, a directional noise monitoring terminal (NMT) is now being developed. This NMT uses directional microphones both to estimate the aircraft direction and to filter out the background noise and ground reflections from the sound pressure level recording.

The objective of this Master thesis is to carry out a theoretical and experimental study on different methods to generate directional microphones for measurement purposes. The main outcome of the study should be a description of the performance characteristics - i.e. frequency response, directivity pattern and signal-to-noise ratio - associated to each method.

Trondheim, June 2014

Sebastià V. Amengual Garí

# Acknowledgements

I would like to thank my supervisors Peter Svensson, Meritxell Genescà and Albino Nogueiras. Specially to Meritxell for all the hours and energy that she spent guiding this thesis and all the feedback received during these months.

I want to thank also Tim Cato for the technical support during this project and Sara Martín for the mathematical input.

Finally, to my parents for their support during all my life.

# Abstract

This thesis deals with the implementation and analysis of different methods to generate a first-order directional microphone for source location and noise measurement purposes. The methods analysed include a cardioid capsule, and virtual methods such the combination of the signals of two omnidirectional microphones, the combination of the signals of an omnidirectional and a figure of 8 microphones, as well as a Soundfield microphone which is based on the Ambisonics principle.

The frequency response function, directivity error and signal-to-noise ratio of the resulting first-order directional microphones have been experimentally studied by implementing each of the methods, performing measurements in the anechoic chamber of the Acoustics Group at NTNU and post-processing the obtained signals using MatLab.

The results obtained from the experiments conclude that the optimum method to generate a first-order directional microphone for measurement purposes at the frequency range of interest of this project (from 80 Hz to 4 kHz) is to use an array of three omnidirectional microphones and combine their signals.

# Contents

# List of Figures

iv

# List of Tables

# Chapter 1

# Introduction

## 1.1   Motivation

The topic of this thesis is directly connected to a project called SOUNDTRACK funded by the European Union's Seventh Framework Programme under the grant agreement num. 299620. In the project SOUNDTRACK a directional aircraft noise monitoring terminal (NMT) is being developed. The goal of this NMT is to provide a measure of the aircraft sound pressure level without background noise contributions. To achieve this the use of first-order directional microphones is planned. With a properly selected directional microphone the contribution from ground borne sources and ground reflections can be noticeably reduced. However, the directivity pattern of the first-order microphone will also weight the aircraft noise level depending on the direction of arrival (DOA) of the aircraft noise. This effect can be compensated if the DOA of the aircraft noise is known. As a consequence, the noise monitoring terminal should also include a system to determine the aircraft noise DOA. At that aim, the final NMT consist of a tetrahedral microphone array with four first-order directional microphones to attenuate the ground reflections and the noise from ground borne sources is used.

The relevant frequency range to estimate the aircraft DOA ranges within 20 Hz and 200Hz because due to atmospheric attenuation, most of the aircraft sound received at the ground -at distances greater than 1 km - is concentrated below 200 Hz. Moreover, below 20Hz the acoustic signal may be severely corrupted by wind noise. On the contrary, the relevant frequency range for aircraft noise monitoing ranges within 200 Hz to 4kHz due to the effect of the A-weighting curve.

The objective of the present thesis is then to experimentally study and compare several existing methods to generate first-order directional microphones with special focus on the two frequency ranges of interests for the SOUNDTRACK project.

## 1.2 Objectives and limitations

The objective of the project is to carry out a theoretical and experimental study on different methods to generate directional microphones for measurement purposes. The project analyzes the performance characteristics (frequency response, directivity pattern and signal-to-noise ratio) of the studied methods.

Although the relevant frequency range of interest starts at 20 Hz, in this study the analysis are performed at frequencies greater than 80 Hz. The reason is that the anechoic chamber in which the acoustic measurements are performed has a cutoff frequency of 80 Hz and the results obtained at frequencies under 80 Hz would not be reliable.

Since the number of first-order directivity patterns is unlimited, in this project the experiments are focused on the study of the cardioid and figure of 8 patterns of microphones generated with the following methods:

- Combination of two pressure (omnidirectional) microphones. Three post-processing techniques are studied in this case: combination of a virtual omnidirectional and figure of 8 microphone signals, combination of virtual back-to-back cardioid signals, and delay and sum of the signals.

- Combination of an omnidirectional and a figure of 8 microphone

- Cardioid microphone capsule

- Generation of a virtual cardioid microphone using the signals from an ambisonics soundfield microphone.

## 1.3 Structure of the report

The structure of this report is divided into six chapters. Chapter 2 contains the theoretical concepts regarding to microphones and directivity patterns classification. Chapter 3 describes the different methods to generate first-order directional microphones used in this project. Chapter 4 explains how the diferent tested methods have been implemented and describes the experimental test procedure. Chapter 5 presents the results and Chapter 6 discusses about the performance of the analyzed methods. Finally, Chapter 7 contains a conclusion of the work developed in this thesis. Annexes A and B contain technical information about the used equipment and the computer code, respectively.

# Chapter 2

# Theoretical concepts

## 2.1 Basic concepts about microphones

### 2.1.1 Definition

A microphone is a transducer capable of sensing changes in air pressure and converting them into an electric signal. A flexible membrane called diaphragm converts the changes in air pressure to mechanical movements and after that, these mechanical movements are converted to an electrical signal [1, pp.68-69]. Depending on the type of microphone, different conversion methods are used.

### 2.1.2 Direction of incidence

The direction of incidence of the sound is defined by two angles measured from the microphone's main axis and it is defined by azimuth $\phi$ and elevation $\gamma$ angles, as seen in Figure 2.1. But since the characteristics of a microphone are usually rotationally symmetric around the main axis, the azimuth angle $\phi$ is in general enough to define the microphone characteristics [2, pp.17]. This angle is called angle of incidence.
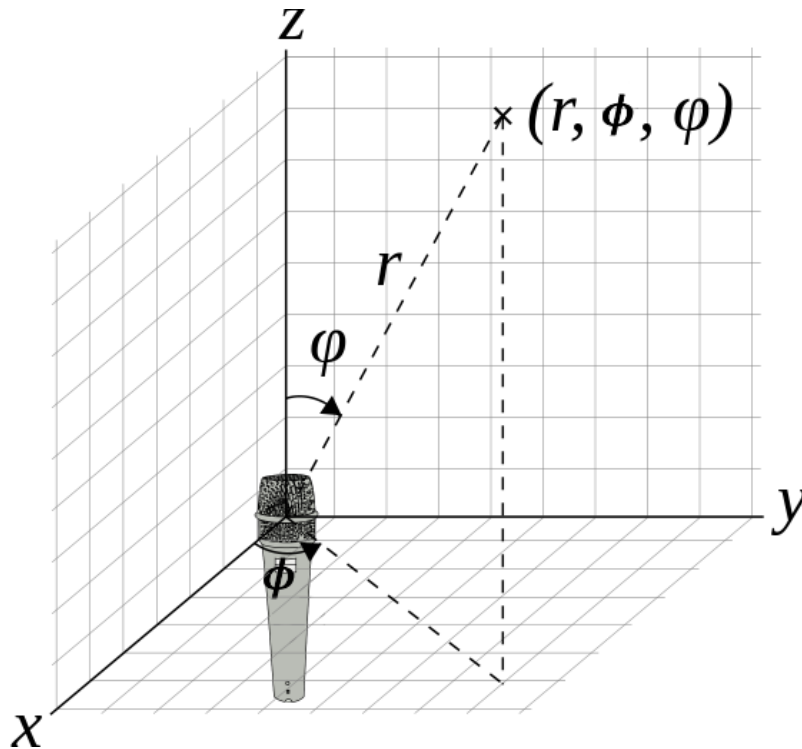
Figure 2.1: Direction of incidence

### 2.1.3 Self-noise

The conversion from air pressure to electrical signal is accompanied by the introduction of some electrical noise. This electrical noise is called microphone self-noise and it is quantified as the acoustical noise that would generate the same output noise level. The spectrum of the self-noise is typically flat, except with equalized unidirectional microphones, in which the magnitude of the self-noise increases towards low frequencies [1, pp.74].

The level of the self-noise in the current microphones is quite low and it is only relevant when the acoustic conditions are very quiet or the dynamic range to cover is very large. It should be taken into account too when using microphone arrays, since the self-noise limits the maximum directivity of the array [1, pp.74].

### 2.1.4 Sensitivity

The sensitivity of a microphone is the voltage output level produced by an input pressure level. The sensitivity is measured in [V/Pa]. The sensitivity of a directional microphone depends both on the frequency and on the angle of incidence of the sound [1, pp.73].

### 2.1.5   Frequency response

The magnitude and phase of the frequency response of a microphone represents the changes of the microphone sensitivity and phase shift as a function of the frequency for a specific angle of incidence [1, pp.75]. It is usually expressed between 20 Hz and 20 kHz (see Figure 2.2), corresponding to the human range of audition. Often the term frequency response is used to refer only to the magnitude while the term phase response is used for the phase. This convention is also used from now on in this text.
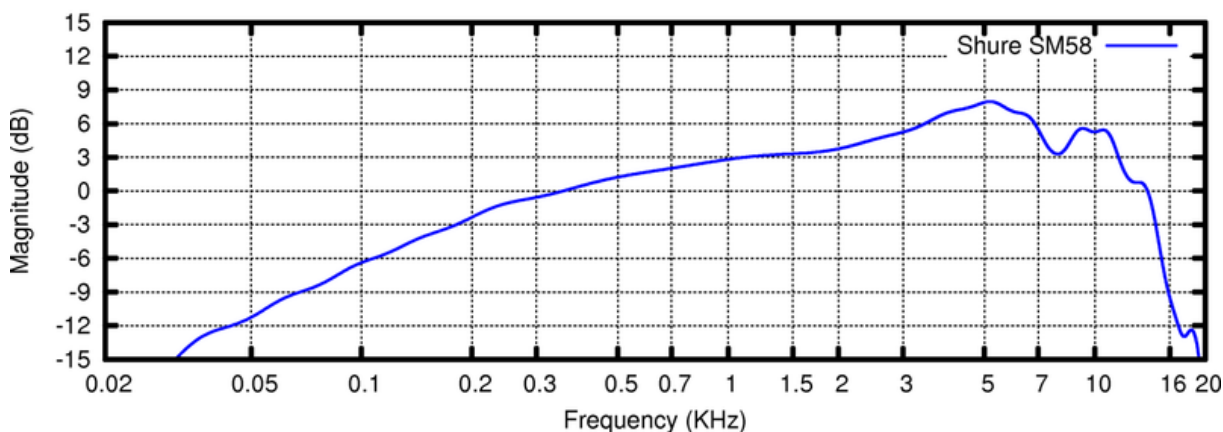


Figure 2.2: Frequency response of a Shure SM58 cardioid microphone

### 2.1.6   Directivity pattern

The magnitude and phase of the directivity pattern represents the microphone sensitivity and phase shift respectively as a function of the incident angle for a particular frequency [1, pp.74-75].

The directivity pattern can be defined as $D(f,d)$, where the variable $d$ is the source position. The distance $\rho$ between the source and the microphone and the direction of incidence are contained in $d = \{\phi, \gamma, \rho\}$ [2, pp.18]. Often the term directivity pattern is used to refer only to the magnitude of $D(f,d)$. This convention is also used from now on in this text.

This thesis focuses in the case where the distance between the sound source and the microphone is large and therefore the sound can be considered a plane wave [1, pp.75]. Taking this assumption into account, the magnitude of the directivity pattern can be represented as a three dimensional function for every frequency of interest, as shown in Figure 2.3.
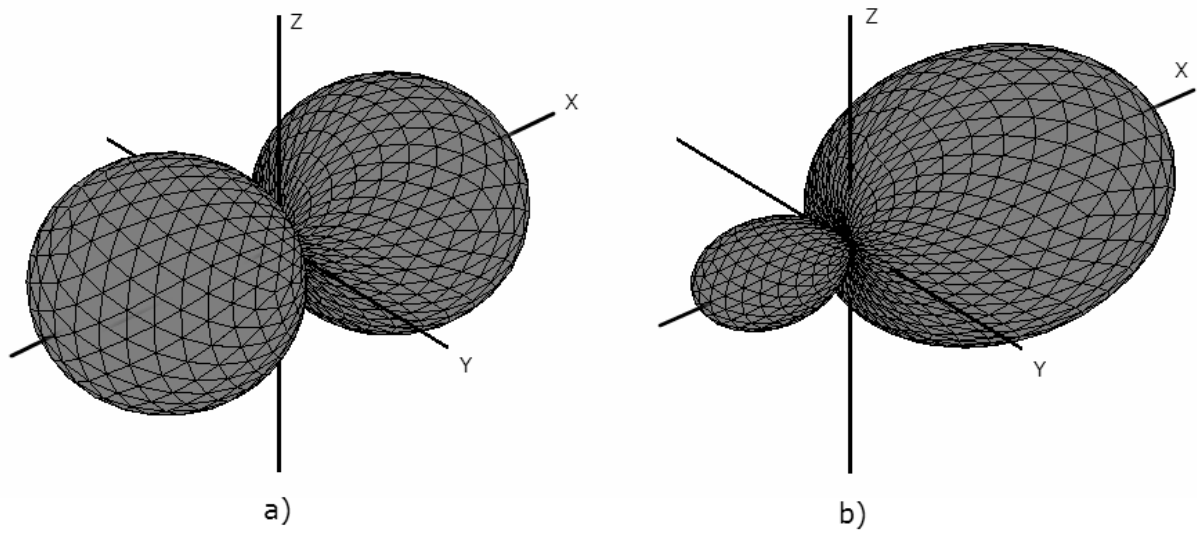
Figure 2.3: 3D directivity patterns represented as a function of the direction of incidence

Moreover, assuming rotational symmetry around the main response axis X one angular dimension can be omitted. Therefore, the directivity can be plotted as a function of the incident angle only in a 2D graph such the one shown in Figure 2.4.
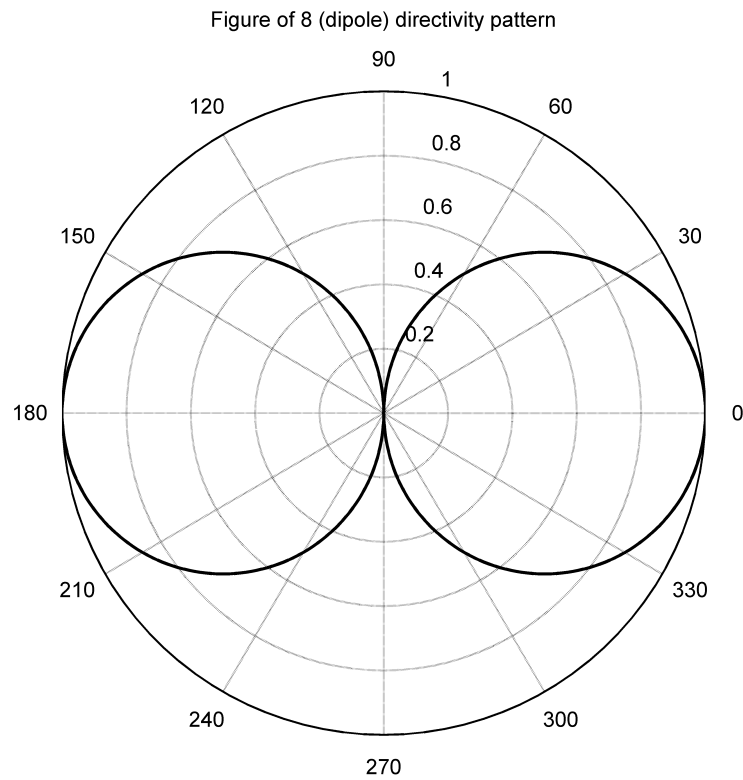
Figure 2.4: Same directivity pattern as Fig. 2.3 a) plotted as a function of the angle of incidence only

Also then, a 3D graphic can show the directivity pattern response of a microphone for different frequencies and angles of incidence as shown in Fig. 2.5.
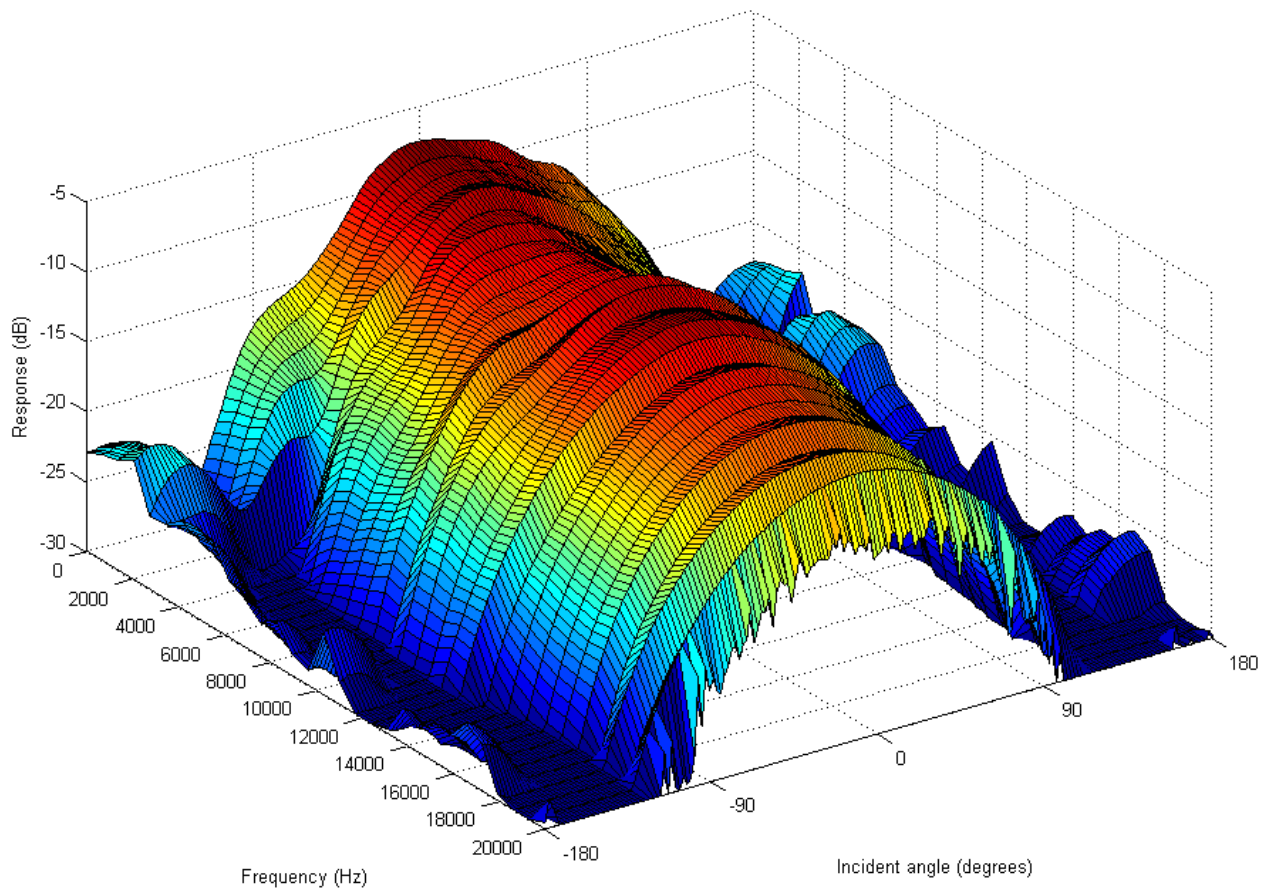
Figure 2.5: Directivity pattern similar to the one plotted in Fig. 2.3 b) represented as a function of frequency and angle of incidence

## 2.2 Microphone Classification by Directivity

Independently from the physical principle used for converting the pressure variations to an electrical signal, a microphone can have different directivity patterns. In general, the directivity of a microphone is determined by the shape of the capsule and the construction method used.

### 2.2.1 Omnidirectional microphone

An omnidirectional microphone has the same sensitivity at every direction, regardless of the angle of incidence of the sound as shown in Fig 2.6. This is achieved by using a capsule

that only exposes the frontal part of the diaphragm to the sound field and the pressure in the interior of the capsule remains constant [2, pp.19]. Usually, small holes are present in the back of the capsule to equalize the atmospheric pressure and the pressure in the interior of the capsule [1, pp.70].

Omnidirectional microphones usually present a flat frequency response from 20 Hz to 20 kHz [1, pp.70].

Omnidirectional directivity pattern
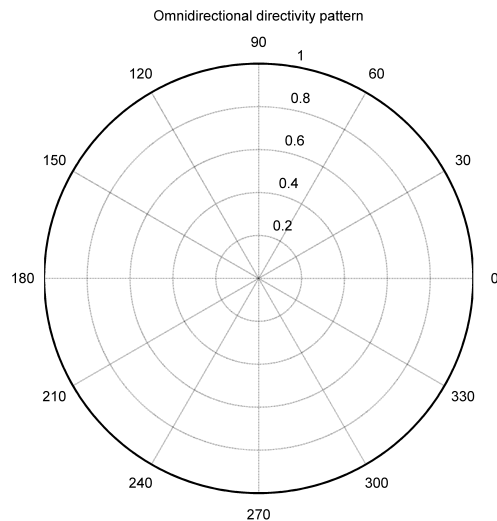
Figure 2.6: Omnidirectional directivity pattern

## 2.2.2   Pressure gradient microphone

A pressure gradient microphone measures the difference of air pressure between two points [3, pp.193]. This means that it is sensitive to the direction of incidence of the sound wave having a directivity pattern known as "figure of 8" or dipole [1, pp.71-72] as seen in Figure 2.4.
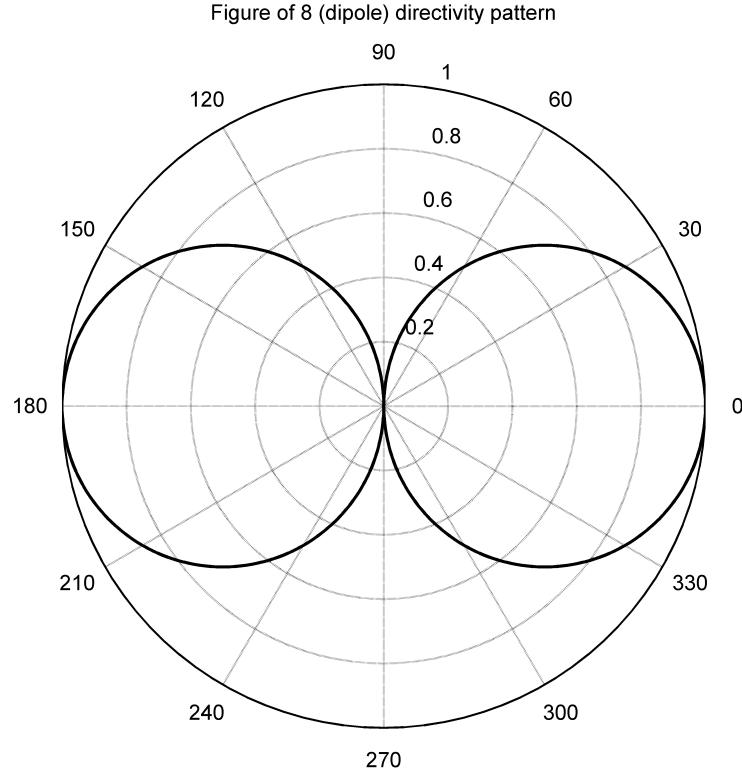
Figure 2.7: Figure of 8 (dipole) directivity pattern

A pressure gradient microphone is sensitive to sounds coming from a direction parallel to its main axis but not to sounds coming from a perpendicular direction. To achieve this directivity pattern the diaphragm is placed inside a capsule open at both ends [2, pp.21-22].

The output signal of a pressure gradient microphone is the difference between the signal at one side of the diaphragm and the same signal at the other side, delayed due to the length of the microphone and the incident angle [1, pp.71]

$$U(f, \phi) = 1 - exp\left(-j2\pi f \frac{l cos \phi}{c}\right) \tag{2.1}$$

where $f$ is the frequency, $c$ is the speed of sound and $l$ is the length of the microphone.

Equation 2.1 can be also expressed as

$$U(f, \phi) = 1 - cos\left(\frac{2\pi \cos(\phi)l}{\lambda}\right) + \sin\left(\frac{2\pi \cos(\phi)l}{\lambda}\right) \tag{2.2}$$

10

where $\lambda$ is the wavelength. If $l << \lambda$ then

$$cos\left(\frac{2\pi \cos(\phi)l}{\lambda}\right) \approx 1 \tag{2.3}$$

$$\sin\left(\frac{2\pi \cos(\phi)l}{\lambda}\right) \approx \frac{2\pi cos(\phi)l}{\lambda}. \tag{2.4}$$

Therefore

$$U = \frac{2\pi \cos(\phi)l}{\lambda} = \frac{2\pi f}{c}l\cos(\phi). \tag{2.5}$$

The frequency response of a pressure gradient microphone is proportional to the cosinos of the angle of incidence and the frequency with an increase of sensitivity of 6 dB/octave [1, pp.72]. A first-order low-pass filter with a frequency response of $\frac{c}{2\pi fl}$ is usually used with pressure gradient microphones in order to achieve a flat frequency response [2, pp.22].

## 2.2.3 First-order directional microphone

A first-order directional microphone has a directivity pattern defined by [4]

$$U(\phi) = b + (1-b)cos(\phi). \tag{2.6}$$

The directivity pattern of a first-order microphone can be adjusted by modifying the value of the parameter $b$ between 0 (figure of 8 microphone) and 1 (omnidirectional microphone) [1, pp.82].

It is important to note that Eq. 2.6 is composed by the sum of directivity patterns of an omnidirectional microphone and a figure of 8 microphone (after compensating the frequency response). Figure 2.8 shows different directivity patterns depending on the value of the parameter $b$ [5, pp.9]. The corresponding values of the parameter $b$ for the most common first-order patterns are shown in Table 2.1.

| Type | $b$ |
|---|---|
| Omnidirectional | 1.00 |
| Sub-Cardioid | 0.75 |
| Cardioid | 0.5 |
| Super-Cardioid | 1/3 |
| Hyper-Cardioid | 0.25 |
| Figure of 8 | 0 |

Table 2.1: First-order directivity microphones
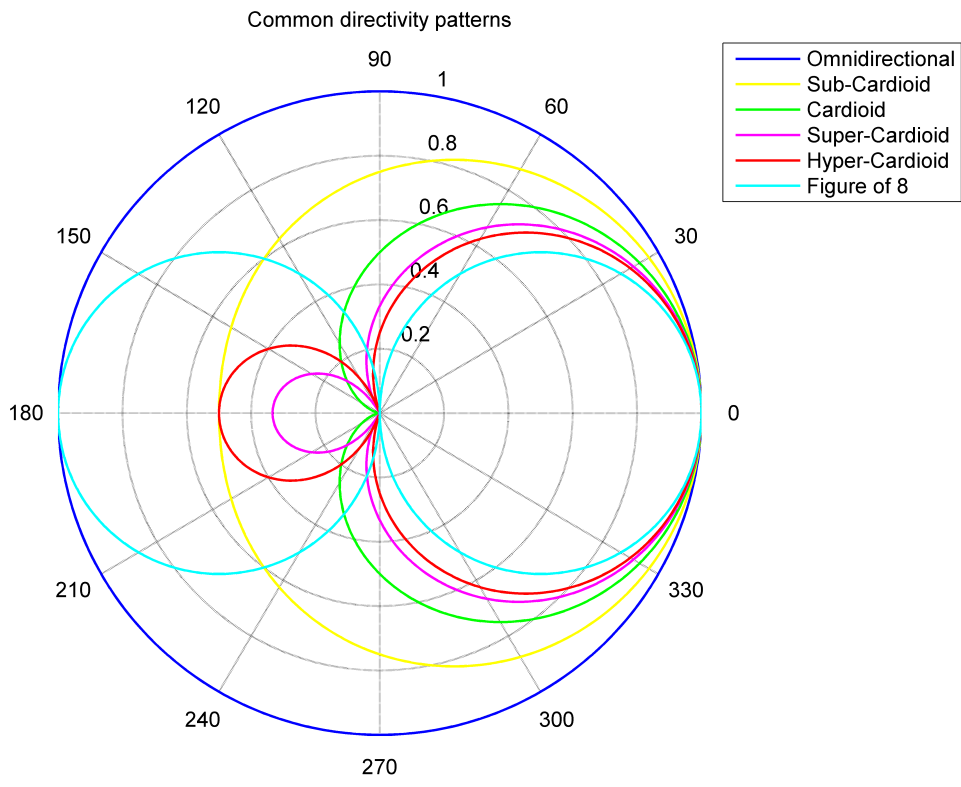
Figure 2.8: Omnidirectional and first-order directivity patterns

# Chapter 3

# Methods to generate a first-order microphone

There exist several methods for creating a first-order microphone, and as it is explained in the previous sections, the objective of this project is to carry out an experimental analysis and a comparison between the different methods. These method can be divided in physical methods (Section 3.1) in which the microphone capsule is designed to provide a particular directivity, and virtual methods (Section 3.2 to 3.4) in which the desired directivity is achieved by combining the signals of a set of microphones.

## 3.1 Directional microphone capsules

There are two methods for generating a first-order microphone by building a modified capsule (see Figure 3.1). These are the most used methods in commercial first-order microphones.

The first method consists commonly of creating a capsule with one side of the diaphragm completely exposed to the sound field and an aperture on the other side of the capsule, partially exposing the other side of the diaphragm. The size of this aperture will determine the parameter $b$ [2, pp.25].

The second method consists of a capsule open on both sides with a non-centered membrane. The sound will reach the rear part of the membrane with a certain delay compared to the front side. In this case, the $b$ parameter is modified by the difference of distance between the diaphragm and the apertures of the capsule [2, pp.26].
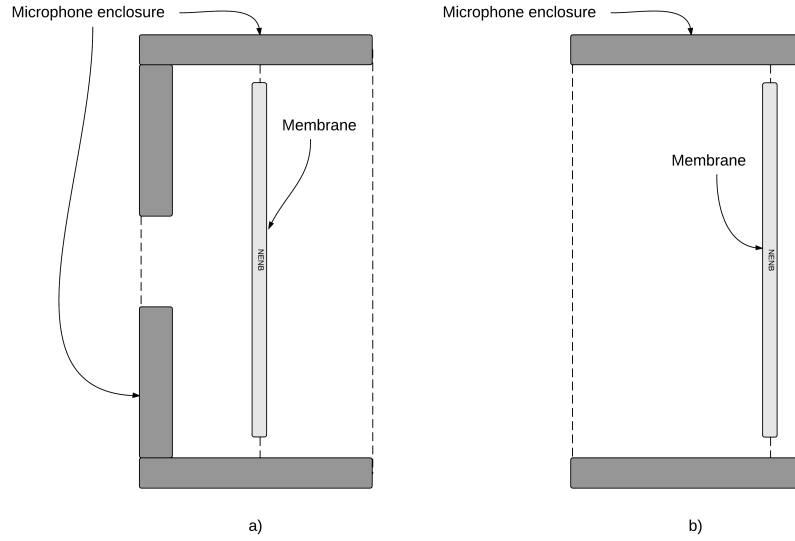
Figure 3.1: a) capsule with a partially exposed membrane, b) open capsule with a displaced membrane

## 3.2   Combination of an omnidirectional and a figure of 8 microphone

As seen in Section 2.2.3, the directivity pattern of a first-order microphone corresponds to the weighted sum of the directivity pattern of an omnidirectional and a figure of 8 microphones. In the same way, a first-order virtual microphone can be obtained by the weighted addition of the signals of an omnidirectional and a figure of 8 microphone. When using this method to generate a new virtual microphone it is important to note that the position of the two microphones must be the same and the figure of 8 microphone should have a frequency correction system. The output of the virtual microphone will then be obtained as

$$P_b(\omega) = bP_{omni}(\omega) + (1-b)P_{fig8}(\omega) \tag{3.1}$$

where $P_b(\omega)$ is the frequency spectrum of the virtual microphone, $P_{omni}(\omega)$ is the frequency spectrum of an omnidirectional microphone and $P_{fig8}(\omega)$ is the frequency spectrum of a figure of 8 microphone [3].

## 3.3 Combination of two omnidirectional microphones

### 3.3.1 Virtual omnidirectional and figure of 8 method

As said in Section 3.2, a first-order microphone can be created by a weighted addition of the signals from an omnidirectional and a figure of 8 microphone. A pair of collocated omnidirectional and figure of 8 microphones can be virtually created using the signals coming from two omnidirectional microphones placed in close positions [6, pp.188-191].

The diagram in Figure 3.2 shows the basic signal combination coming from two omnidirectional microphones separated by a distance L. The coefficients of the filters $H_1$ and $H_2$ determine the directivity pattern of the resulting virtual microphone, and the response of the filter $H_0$ determines the frequency response of the virtual microphone.
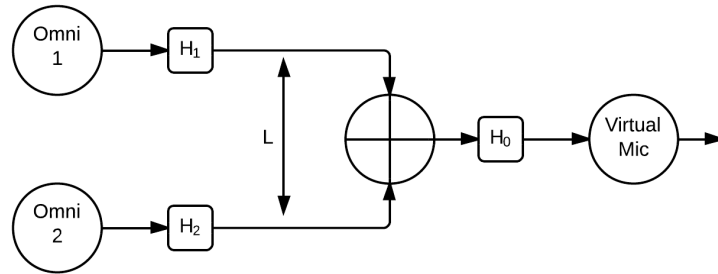


Figure 3.2: Basic diagram of the generation of an omnidirectional or figure of 8 virtual microphone from omnidirectional signals

It is useful to define $p_{mid}$ as the pressure present at the middle point between the two omnidirectional microphones

$$p_{mid} = p_1 \exp^{-jk\frac{L}{2}cos\phi} = p_2 \exp^{-jk\frac{L}{2}cos\phi} \tag{3.2}$$

where $p_1$ and $p_2$ are the pressure received by the microphones 1 and 2 respectively and $k$ is the wavenumber ($\frac{2\pi}{\lambda}$).

In order to obtain a first-order microphone the following procedure must be followed:

- Create a virtual omnidirectional microphone in the central position between the two real microphones. To do this the response of $H_1$ and $H_2$ must be equal to 0.5. This will guarantee an equal contribution from both omnidirectional microphones. Since the frequency response of a pressure microphone is flat, the response of $H_0$ must be 1 [6, pp.189].

  If the filters are built using the specified coefficients, the resulting signal will be

15

$$y = 0.5(p_1 + p_2) = 0.5 p_{mid} \left( \exp^{jk\frac{L}{2}\cos\phi} + \exp^{-jk\frac{L}{2}\cos\phi} \right) = p_{mid}\cos\left(\frac{kL\cos\phi}{2}\right). (3.3)$$

Taking into account that the distance between the microphones is much smaller than the wavelength ($kL << 1$) the output response can be approximated as

$$y \approx p_{mid} \tag{3.4}$$

- Create a virtual figure of 8 microphone in the central position between the two real microphones. Creating a figure of 8 microphone can be achieved by subtracting the signal of one omnidirectional microphone to the other one. It means that in this case the values of the filters are $H_1$=1 and $H_2$=-1 or $H_1$=-1 and $H_2$=1. As explained in Section 2.2.2, the response of a pressure gradient (or figure of 8) microphone is not flat, and in order to compensate this response, the filter $H_0$ must have a low-pass response equal to $\frac{1}{jkL}$ [6, pp.190].

If in Equation 3.2 the distance between the microphones is much smaller than the wavelength ($kL << 1$) then

$$p_1 \approx p_{mid}\left(1 + j\frac{kL\cos\phi}{2}\right) \tag{3.5}$$

$$p_2 \approx p_{mid}\left(1 - j\frac{kL\cos\phi}{2}\right). \tag{3.6}$$

Combining the two input signals

$$y = H_0\left(H_1 p_1 + H_2 p_2\right) \approx H_0 p_{mid}\left[1 + j\frac{kL\cos\phi}{2} - \left(1 - j\frac{kL\cos\phi}{2}\right)\right] = p_{mid}\cos\phi (3.7)$$

- Once the two virtual microphones are created, the last step is to combine the signals of the virtual microphones in order to obtain a first-order microphone, as explained in Section 3.2. The full diagram of the process is shown in Figure 3.3
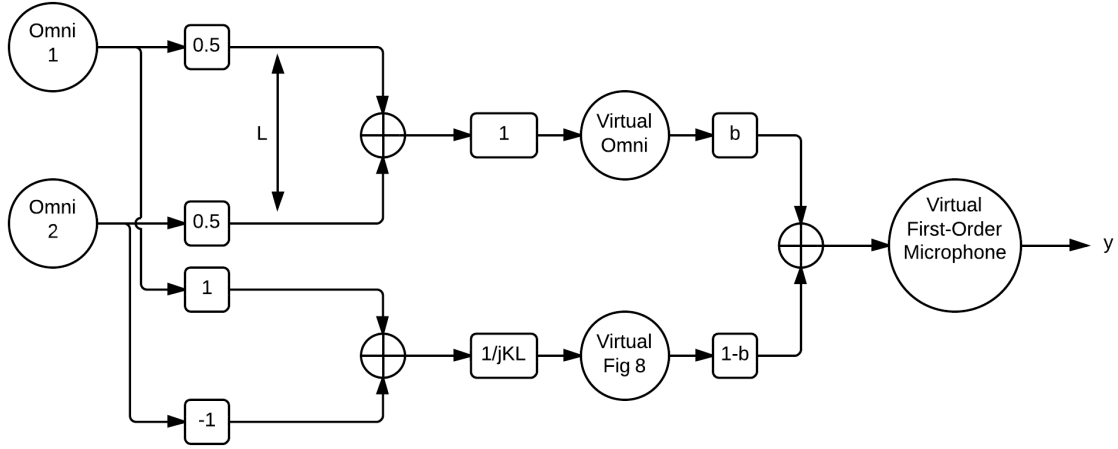
Figure 3.3: Virtual omnidirectional and figure of 8 method

## 3.3.2 Delay and sum method

The delay and sum method consists of the combination of a signal from an omnidirectional microphone with a phase shifted delayed signal from another omnidirectional microphone placed at a close distance L [3]. The diagram of combination of the signals is shown in Figure 3.4.
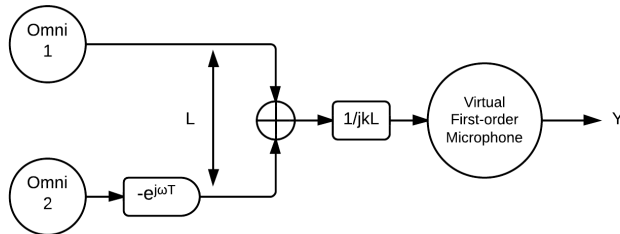


Figure 3.4: Delay and Sum method diagram

For a plane-wave signal s(t) with spectrum $S(\omega)$ and angle of incidence $\phi$, the output signal will be

$$Y(\omega, \phi) = S(\omega)\left(1 - \exp^{-j(\omega T + kL)}\right) = S(\omega)\left(1 - \exp^{-j\omega[T + (L\cos\phi)/c]}\right) \qquad (3.8)$$

where T is the delay applied to one of the signals. In terms of magnitude, the output signal will be

$$|Y(\omega, \phi)| = 2 \left| S(\omega) \sin \frac{\omega[T + (L \cos \phi)/c]}{2} \right|. \tag{3.9}$$

Assuming a small spacing between the microphones and a small delay ($kL << \pi$ and $\omega T << \pi$) the output signal can be expressed as a combination of a constant term and a figure of 8 term giving the possibility of creating any first-order directivity pattern by varying the value of the delay [7].

$$|Y(\omega, \phi)| \approx \omega \left| S(\omega)[T + (L \cos \phi)/c] \right| \tag{3.10}$$

It is important to note that, as in the previous methods, the virtual output has a dependence on the frequency which has to be compensated with a first-order low-pass filter.

The delay necessary for every different pattern is

$$T = \frac{Lb}{c(1 - b)}. \tag{3.11}$$

The values of the parameter $b$ needed to create the different directivity patterns are contained in Table 2.1. As can be observed in the table, to create an omnidirectional microphone the value of $b$ has to be equal to 1, but when this value is substituted in Eq. 3.11 the value of the delay equals infinite meaning that it is not possible to obtain a virtual omnidirectional microphone with this method.

### 3.3.3 Virtual back-to-back cardioid method

The back-to-back method consists of creating two virtual cardioid microphones with inverted patterns (see Figure 3.5) combining the signals of two omnidirectional microphones with a delay and a phase shift. Once the two virtual cardioid microphones are created any first-order directional microphone can be created by a weighted sum of the two virtual signals. The last step is to compensate the frequency response with a first-order low-pass filter in order to obtain a flat response [4].
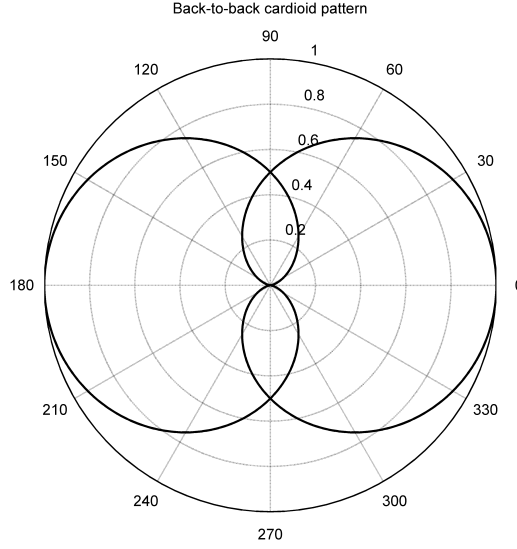
Figure 3.5: Back-to-Back cardioid patterns

Equation 3.9 shows the resulting signal obtained from an omnidirectional microphone and a delayed signal from another omndidirectional microphone placed at a distance L.

If the delay T is set to T=L/c then the combination of the signals gives a cardioid pattern. If the signal processing is performed as depicted in Figure 3.4, the resulting pattern is a so called forward cardioid and if the signals of the two omnidirectional microphones in Figure 3.4 are interchanged then the result is a so called backwards cardioid

$$|C_F(\omega,\phi)| = 2\left|S(\omega)\sin\frac{kL(1+\cos\phi)}{2}\right| \tag{3.12}$$

$$|C_B(\omega,\phi)| = 2\left|S(\omega)\sin\frac{kL(1-\cos\phi)}{2}\right| \tag{3.13}$$

where $C_F(\omega,\phi)$ and $C_B(\omega,\phi)$ are the directivity patterns of a forward and a backward facing cardioid respectively, L is the distance between the microphones and k is the wavenumber $(\frac{2\pi}{\lambda})$. The directivity pattern of the back-to-back cardioid microphones created is shown in Figure 3.5.

The subtraction of the signals from the back-to-back cardioids with a weighting parameter $\beta$ on the forward cardioid signal gives

$$|Y(\omega,\phi)| = S(\omega)2\left|\sin\frac{kL(1+\cos\phi)}{2} - \beta\sin\frac{kL(1-\cos\phi)}{2}\right| \tag{3.14}$$

19

If the distance between the microphones much smaller than the wavelength ($kL << 1$), Equation 3.14 becomes

$$|Y(\omega, \phi)| \approx S(\omega)kL\left[b + (1 - b)\cos\phi\right] \tag{3.15}$$

wich equals the response of a first-order directional microphone. Note that the resulting signal needs to be corrected with a first-order low-pass filter with response $\frac{1}{jkL}$.

The complete diagram showing the combination of the signals, the value of the filters and the value of the delay can be seen in Figure 3.6 [7].
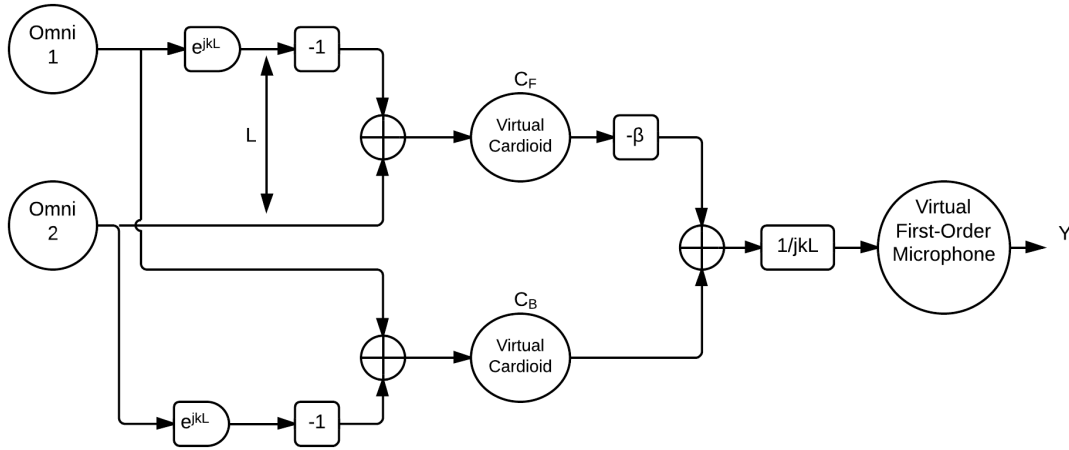


Figure 3.6: Back-to-Back method diagram

## 3.4 Ambisonics

The ambisonics format or B-format is a first-order recording format composed by the signals of four cardioid microphone capsules $L_B$, $L_F$, $R_B$ and $R_F$ mounted inside a tetrahedron and oriented to the different sides of the structure. The four capsules are identical single-diaphragm cardioids and their directivity patterns are well defined at all frequencies. The signals from the capsules are known as A-format and their combination gives as a result four signals called W, X, Y and Z corresponding respectively to an omnidirectional microphone, and a front-back, a left-right and an up-down sound pressure gradient microphone (figure of 8) [8]

$$\begin{aligned}
W &= L_F + R_B + R_F + L_B \\
X &= L_F - R_B + R_F - L_B \\
Y &= L_F - R_B - R_F + L_B \\
Z &= L_F + R_B - R_F - L_B.
\end{aligned} \tag{3.16}$$

20
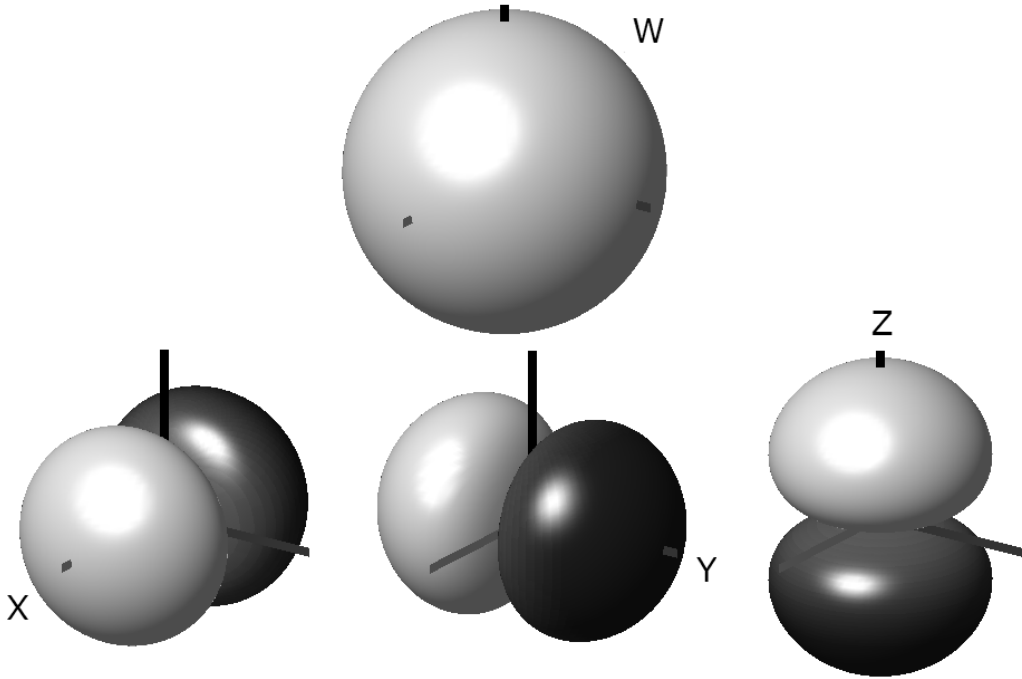
Figure 3.7: W, X, Y and Z ambisonics signals directivity patterns

The directivity patterns of the B-format signals shown in Figure 3.7 are defined by the following expressions [6, pp.165]

$$W(\omega) = S(\omega)\frac{1}{\sqrt{2}}$$
$$X(\omega, \phi, \gamma) = S(\omega)\sin\phi\cos\gamma$$
$$Y(\omega, \phi, \gamma) = S(\omega)\sin\phi\sin\gamma \qquad (3.17)$$
$$Z(\omega, \phi) = S(\omega)\cos\phi.$$

By combining the signals of an ambisonics device it is possible to obtain any first-order directivity pattern and the maximum directivity direction can be chosen. To achieve this, it is necessary to perform a weighted sum of the different signals. The value of the parameters $a$, $b$, $c$ and $d$ will determine the direction of the maximum of sensitivity and the shape of the pattern [6, pp.165].

$$U(\phi, \gamma) = \frac{a}{\sqrt{2}} + b\sin\phi\cos\gamma + c\sin\phi\sin\gamma + d\cos\phi \qquad (3.18)$$

# Chapter 4

# Experiments

## 4.1 Implementation of the methods

This section contains the main information regarding the specific sensors used to evaluate each of the methods described in Chapter 3. More technical information regarding to the equipment used for the experiments is given in the appendix A

### 4.1.1 Directional microphone capsule

To analyse the performance of a first-order directional capsule a condenser AKG C460B microphone has been used. It includes an AKG CK1 capsule and a preamplifier. The capsule is designed to provide a permanent cardioid directivity pattern. Since this is a condenser microphone it needs a phantom supply. The preamplifier used with this microphone was a Shure FP23 with a configuration of 48 V of phantom supply and 50 dB of gain. The usable frequency range of the set is from 20Hz to 22kHz. This equipment is shown in Fig. 4.1

The frequency response and directional chracteristics characteristics of the microphone have been measured directly without further post-processing.



Figure 4.1: Shure FP23 preamplifier & AKG C460B

### 4.1.2 Combination of an omnidirectional and a figure of 8 microphone

An acoustic vector sensor is composed by a pressure microphone and three particle velocity sensors oriented in the X,Y and Z directions. Each velocity sensor measures the projection of the particle velocity on its own axis. Therefore, the output of each velocity sensor is proportional to the cosine of the angle between the particle velocity and the velocity sensor axis providing a figure of 8 directivity pattern. As a consequence, using the pressure signal which is omnidirectional and one of the velocity signals it is possible to create a first-order microphone following the method explained in Section 3.2.

The device used in the experiments is a Microflown USP-Regular probe with a flat frequency range from 10Hz to 10kHz. The probe is equipped with a 4-channel signal conditioner MFSC4, which includes a filter and a preamplifier for correcting the response and the gain of the velocity sensors. The signal conditioner modifies the input signal in order to get a similar frequency response from the pressure sensor and the velocity sensors. The mentioned equipment is shown in Fig. 4.2.



Figure 4.2: MSCF4 signal conditioner & Microflown USP sensor

### 4.1.3 Combination of two omnidirectional mirophones

To implement the methods described in Section 3.3 a set of two G.R.A.S 40AI microphones is used. These are omnidirectional microphones designed to have matched phases, which means that the response of the two microphones is virtually the same. This set of microphones guarantees a flat frequency response ($\pm 1$ dB) from 2.5 Hz to 10 kHz.

Since these are condenser microphones they need a preamplifier and power supply. The preamplifier connected to every G.R.A.S. capsule is a Norsonic 1201 and the amplifier used for providing the power supply is a two channel Norsonic 336.

As explained in Section 3.3, the distance between the omnidirectional microphones is an important factor for creating a virtual microphone. For this reason, the matched microphones were placed at different distances - 10.44 mm, 23.49 mm, 43.84 mm and 98.35 mm - in order to analyze the influence of the distance on the generated virtual

microphones. As it can be seen in Fig. 4.3 microphone spacers such the ones used for sound intensity measurements were used to ensure an accurate separation and alignment between the microphones
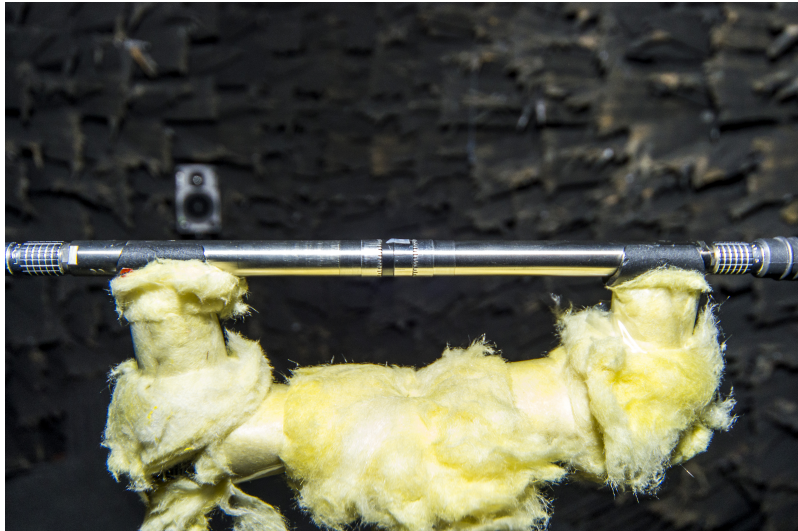


Figure 4.3: G.R.A.S. 40AI microphones set-up

## 4.1.4 Ambisonics Soundfield microphone

The device used to create a virtual cardioid microphone using the Ambisonics method was a Soundfield SPS422B Microphone System composed by an ambisonics microphone and a processor unit to obtain the desired directivity pattern (see Figure 4.4). The processor provides 6 output signals: W which is an omnidirectional pressure signal; X,Y and Z which are pressure signals with a figure of 8 directivity oriented as the correspondent axis; and two equal signals with first-order directivity labelled Left and Right.



Figure 4.4: Soundfield SPS422B Microphone System

The processor unit allows the user to select the output directivity pattern and the direction of the maximum of sensitivity of the signals Left and Right. Since the processor can be configured to provide a Mono signal only one of the processed outputs is necessary to obtain a first-order microphone. The selectors allows the user to select any value of the parameter $b$ from 0 to 1. In this test, the selected value was $b=0.5$ in order to obtain a cardioid microphone at the output.

## 4.2   Set-up and measurement procedure

The measurements were performed between the 3rd and the 6th of March and between the 5th and the 7th of May 2014 in the anechoic chamber of the Acoustics Group of the Department of Electronics and Telecommunication at the Norwegian University of Science and Technology.

The dimensions of the anechoic chamber are $6.65 \times 8.40 \times 6.65$ meters and its cutoff frequency is 80 Hz. The anechoic chamber is equipped with a thermometre and the temperature readings are used to calculate the speed of sound for each particular test.

In order to obtain the directivity pattern of a microphone it is necessary to perform several measurements at a different angles of incidence. For this purpose, the different microphones were mounted on a Norsonic Nor265 turntable placed aproximately at the center of the room. The acoustic source used in the experiments was a Genelec 1029A, a two-way active loudspeaker placed at one corner of the room. The distance between the source and the tested microphones was 2.2 meters. A sketch of the set-up can be observed in Figure 4.5.
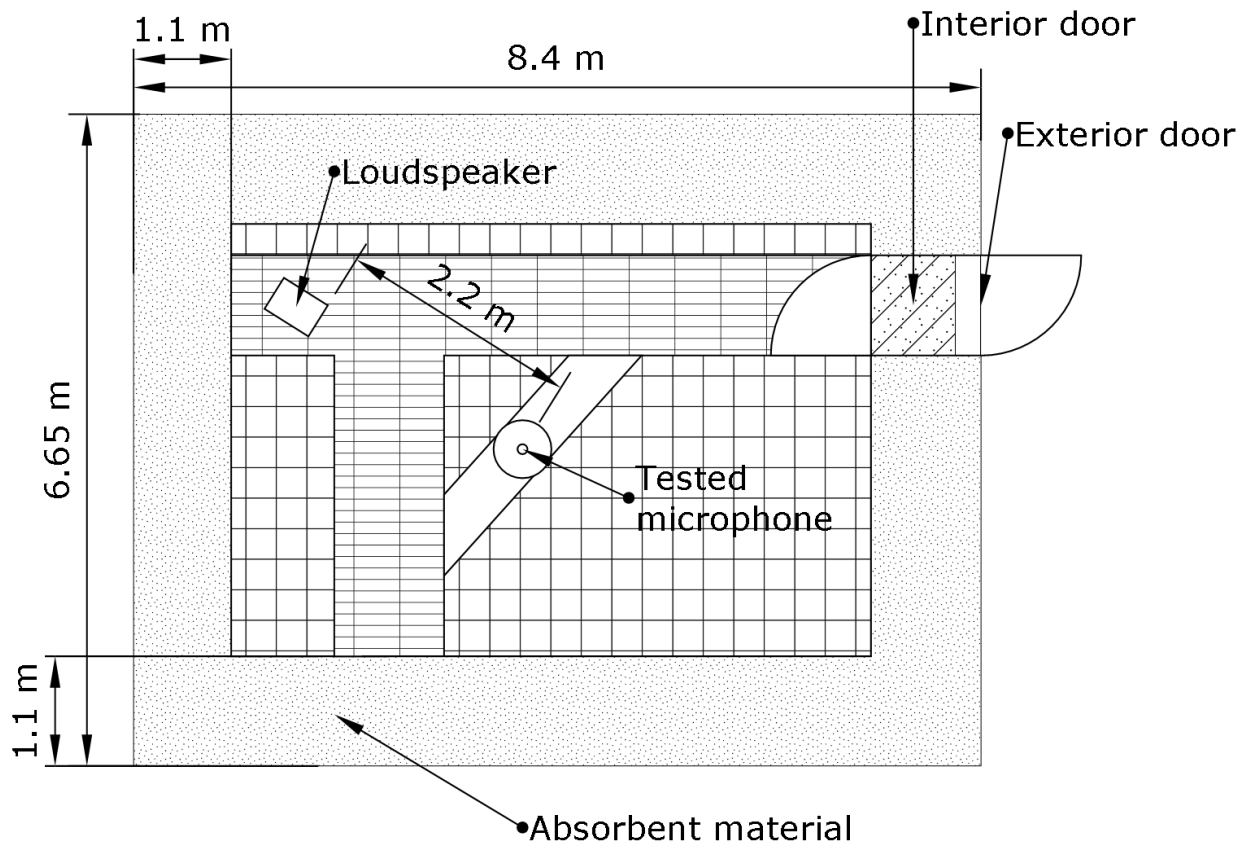
Figure 4.5: Drawing of the set-up mounted in the anechoic chamber

The tested microphone (or array) was placed at approximately 1.5 meters over the wire mesh floor of the chamber. The height of the set-up was slightly modified depending on the analyzed element and its subjection method. A gloval view of the set-up can be seen in Fig. 4.6.
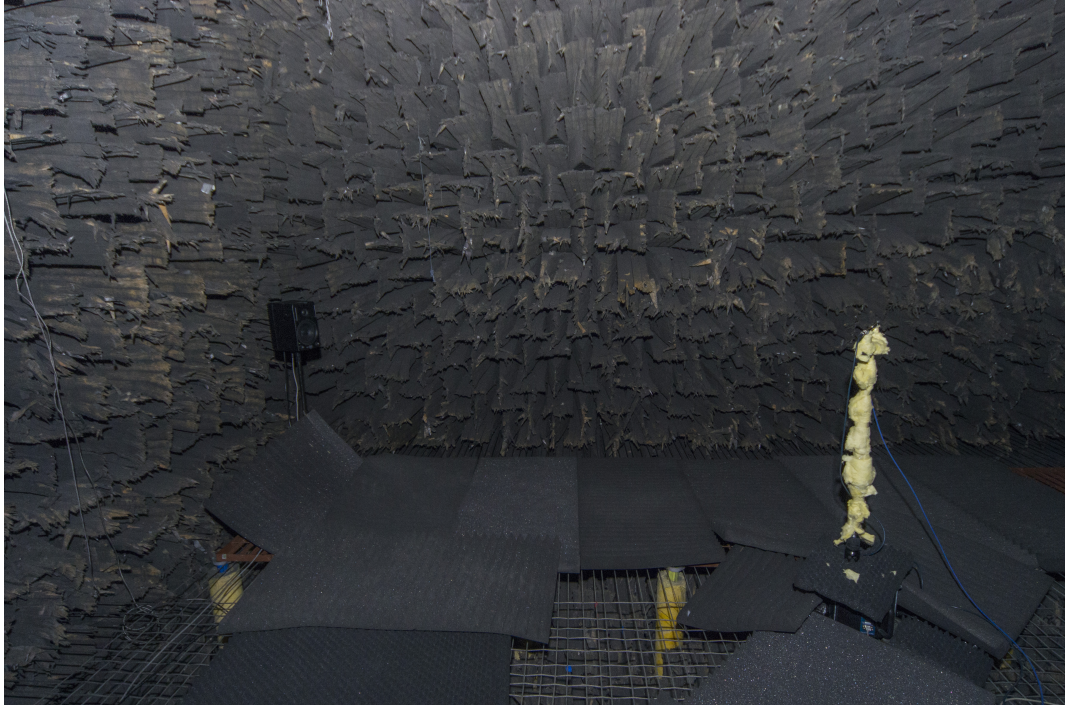
Figure 4.6: Global view of the set-up before performing a measurement

The acquisition and generation system used in the experiments includes a computer equipped with a LynxTWO-C soundcard, and the WinMLS and MatLab software which was placed outside of the anechoic chamber.

The excitation signal was a 4 seconds sinusoidal sweep from 80 Hz to 20 kHz with a sampling frequency of 44100 Hz, in order to avoid aliasing, and digital resolution of 32 bits per sample. The software WinMLS both generates the excitation signal and computes the impulsional response of the individual sensors. These impulsional responses are used later to extract the characteristics of the first-order directional microphones. Several measurements were performed for every tested microphone at different incident angles. The synchronization between the turntable movement, the generation of the excitation signal and the measurement of the impulse response was controlled by a modificable MatLab script, automatizing the measurements.

For each tested microphone or sensor array described in Section 4.1 the measurement procedure was the following:

- Install the test microphone or array on the turntable and align it with the loudspeaker. Since the used source is a two way loudspeaker, the elements were aligned with the tweeter of the loudspeaker. This was done because the wavelength at high frequencies is much smaller than at low frequencies and aligning the tweeter and the receiver increases the precission of the measurement at high frequencies without noticeably affecting the precission of the measurements at low frequencies.

- Cover of the reflecting elements in the anechoic room, such as the gangway, the turntable and the microphone stand as shown in Figures 4.6 and 4.7).

- Register of the room temperature, leave the room and close the door of the anechoic chamber.

- Execute the MATLAB script that governs the automatic measurement routine. This script launches the software WinMLS which simultaneously sends a 4 second sweep sine signal from 80 to 20 kHz to the loudspeaker and computes the impulse response of the test sensor/s. After storing the measured data WinMLS closes and the MATLAB script sends an order to the turntable to turn $2°$. These steps are repeated until the turntable has rotated $358°$.

For every tested microphone or array 180 different measurements were performed covering a range of angles of incidence from $0°$ to $360°$ at $2°$ intervals. Assuming axial simmetry this procedure is apropriate to generate and analyze the 2D directivity patterns of the first-order directional microphones generated using the diferent methods under study. It is important to note also that, for every different setup, a measurement in absense of signal was performed, in order to obtain the self-noise level of the sensors.
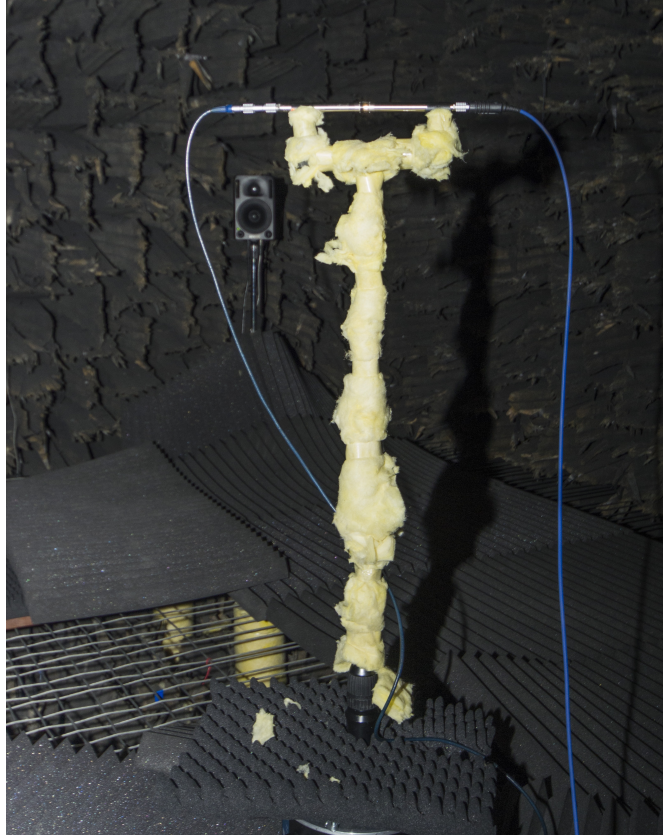
Figure 4.7: G.R.A.S. matched microphones set-up mounted at L=11.04 mm after covering the reflectant elements

## 4.3 Post-processing

In order to characterize the performance of the methods, three parameters are analyzed: the frequency response, the directivity error and the signal-to-noise ratio.

**Computation of the frequency response (FRF)**

The Frequency Response is defined as the sensitivity of the generated first-order directional microphone relative to the sensitivity of an ideal first-order directional microphone averaged over all the incident angles. The Frequency Response Function is determined by a scaling factor $A(\omega)$ as

$$FRF(\omega) = 10 \log \frac{1}{A(\omega)}. \tag{4.1}$$

The factor A($\omega$) has been calculated as follows:

- The starting point is the measured impulsional response of the analyzed microphone measured for every incident angle $IR_\phi(t)$.

- The background noise is removed by performing a zero padding. The obtained response is called $IR'_\phi(t)$.

- After this, the directivity $\hat{D}'_\phi(\omega)$ is obtained by applying a Fourier transform on $IR'_\phi(t)$. It is important to note that the directivity $\hat{D}'_\phi(\omega)$ is influenced by the response of the loudspeaker and the room.

$$\hat{D}'_\phi(\omega) = \sum_{t=0\,s}^{T} IR'_\phi(t)e^{j\omega t}. \tag{4.2}$$

where T is the length in seconds of the impulsional response.

- To remove the influence of the loudspeaker and the room the directivity $\hat{D}'_\phi(\omega)$ is corrected using a reference signal $\hat{D}_{ref_\phi}(\omega)$ that contains the FRF of the loudspeaker and the anechoic chamber

$$\hat{D}_\phi(\omega) = \frac{\hat{D}'_\phi(\omega)}{\hat{D}_{ref_\phi}(\omega)}. \tag{4.3}$$

The scaling factor $A(\omega)$ can be obtained by minimizing the difference between the scaled measured directivity pattern and the ideal directivity pattern

$$\min_{A\in\mathbb{R}} \left( \sum_{\phi=0°}^{358°} \left| A(\omega)\hat{D}_\phi(\omega) - D_\phi(\omega) \right|^2 \right)'. \tag{4.4}$$

where $D_\phi(\omega)$ is a vector containing the theoretical directivity pattern and $\hat{D}_\phi(\omega)$ is a vector containing the measured directivity pattern after removing the loudspeaker and room influence. A mathematical expression of A($\omega$) can be found from

$$\frac{\partial \left( \sum_{\phi}^{358°} \left| A(\omega)\hat{D}_\phi(\omega) - D_\phi(\omega) \right|^2 \right)}{\partial A(\omega)} = 0 \tag{4.5}$$

which leads to

$$A(\omega) = \frac{\sum_{\phi=0°}^{358°} D_\phi(\omega)\hat{D}_\phi(\omega)}{\sum_{\phi=0°}^{358°} \hat{D}_\phi^2(\omega)} \tag{4.6}$$

30

Figure 4.8 shows the graphic representation of the ideal directivity pattern $D_\phi$ computed according to Equation 2.6, and example of the measured directivity pattern $\hat{D}_\phi$ and the scaled measured directivity pattern $A\hat{D}_\phi$ at a single frequency.
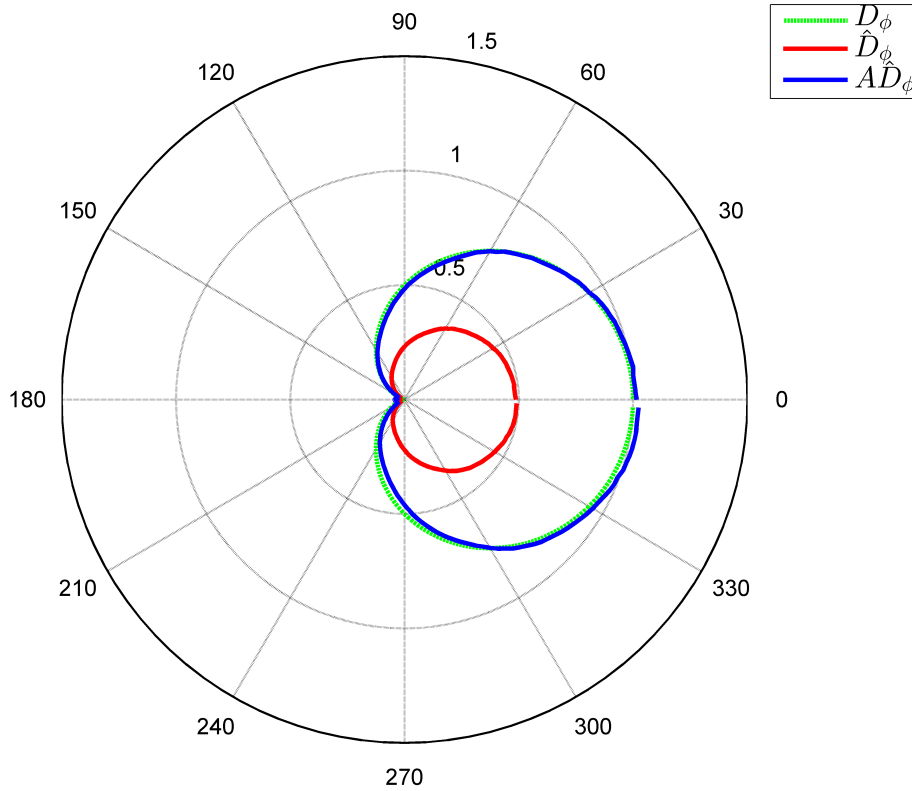


Figure 4.8: Ideal directivity pattern, measured directivity pattern and measured directivity pattern after applying the magnitude correction

**Computation of the Directivity Error**

The directivity error measures the deviation between the directivity pattern of the created first-order directivity microphone and the directivity pattern of an ideal first-order directional microphone after correcting the differences of sensitivity. The chosen parameter for measuring the directivity error is the residual sum of squares integrated over all the measured angles

31

$$\xi(\omega) = \left( \left| \sum_{\phi=0°}^{358°} A(\omega)\hat{D}_\phi(\omega) - D_\phi(\omega) \right|^2 \right).$$ (4.7)

Figure 4.9 shows the difference between an ideal cardioid pattern and a scaled measured pattern. The sum of the squares of this difference for each angle of incidence is the error at a single frequency and a single angle.
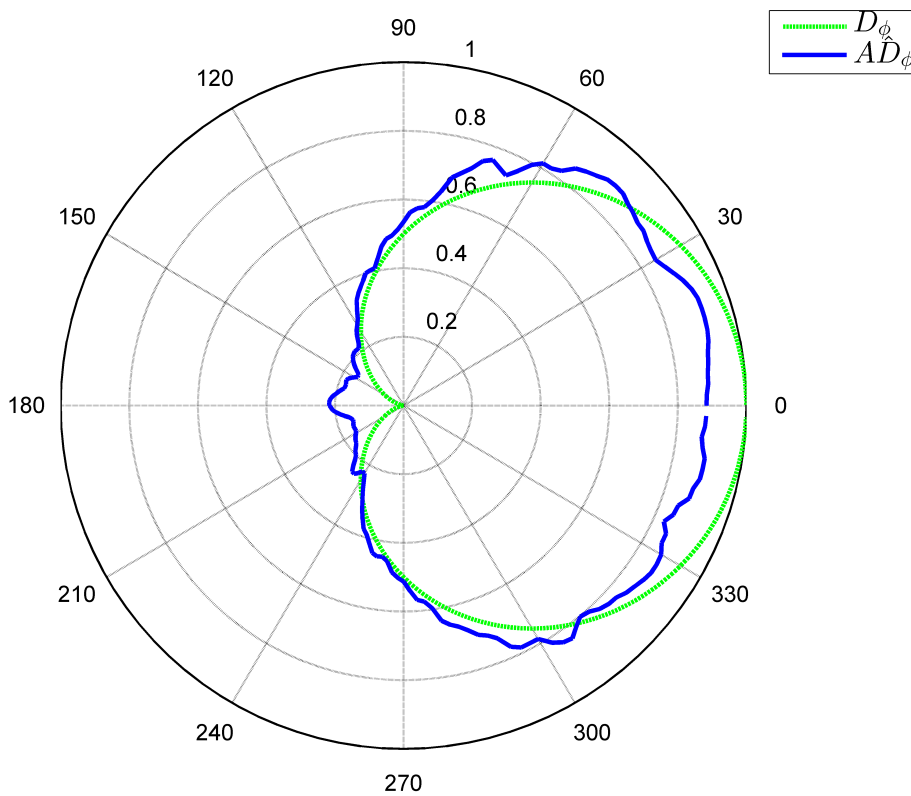


Figure 4.9: Ideal directivity pattern $D_\phi$ and the scaled measured directivity pattern $A\hat{D}_\phi$ of a cardioid microphone

The results of the error are presented as global values for low frequencies (from 80 Hz to 200 Hz), mid frequencies (from 200 Hz to 4 kHz) and high frequencies (from 4 kHz to 20 kHz). The final value of error consists on an average of the error for the selected frequency.

$$\xi_{LF} = \sum_{\omega=80\,Hz}^{200\,Hz} \frac{\xi(\omega)}{N} \qquad \xi_{MF} = \sum_{\omega=200\,Hz}^{4\,kHz} \frac{\xi(\omega)}{N} \qquad \xi_{LF} = \sum_{\omega=4\,kHz}^{20\,kHz} \frac{\xi(\omega)}{N} \qquad (4.8)$$

where $\xi_{LF}$, $\xi_{MF}$, $\xi_{HF}$ are the average errors at mid, low and high frequencies respectively and N is the number of samples of error averaged.

The minimum value of the directivity error is 0, which means that the measured pattern fits perfectly with the ideal pattern. In order to establish a range of quality, Table 4.3 shows the values of the directivity error and the qualitative meaning of every value of directivity error.

| $\xi(\omega)$ | Goodness of fit |
|---|---|
| 0 to 1 | Excellent fit |
| 1 to 5 | Very good fit |
| 5 to 10 | Good fit |
| 10 to 50 | Acceptable fit |
| 50 to 100 | Bad fit |
| > 100 | Very bad fit |

Table 4.1: Qualitative meaning of the directivity error

**Computation of the signal-to-noise ratio (SNR)**

The signal-to-noise ratio represents the relationship between the frequency response in the main axis of the microphone or array and the microphone self-noise

$$SNR(\omega) = 10log\left(\frac{FRF_0^2(\omega)}{N^2(\omega)}\right). \qquad (4.9)$$

where the frequency response on the main axis is computed as

$$FRF_{0°}(\omega) = \sum_{n=1}^{N} IR_{0°}(t)e^{j\omega t}, \qquad (4.10)$$

and the frequency response of the microphone self-noise $N(\omega)$ is calculated from the impulse response measured in absense of signal from the loudspeaker $IR_n(t)$ as

$$N(\omega) = \sum_{\omega=80\,Hz}^{20\,kHz} IR_n(t)e^{j\omega t}. \qquad (4.11)$$

Since $FRF_{0°}(\omega)$ contains also the microphone self-noise it is necessary to compute the signal-to-noise ratio as

$$SNR(\omega) = 10log\left(\frac{(FRF_{0°}^2(\omega) - N^2(\omega))}{N^2(\omega)}\right) = 10log\left(\frac{FRF_{0°}^2(\omega)}{N^2(\omega)} - 1\right). \qquad (4.12)$$

# Chapter 5

# Results

In this section the frequency response, signal-to-noise ratio and directivity error of each of the microphones or sensor arrays described in Chapter 4 are presented. Two directivity patterns have been studied, a cardioid and a figure of eight. Since the directivity pattern of the cardioid capsule is fixed, this one has only been included in the study of the cardioid directivity.

Table 5.1 shows the nomenclature used in this section to refer to the different methods to generate first order directional microphones.

| Name of the method | Abreviation |
| :---: | :---: |
| Directional microphone capsule | Cardioid capsule |
| Combination of an omnidirectional and a figure of 8 microphone | AVS-Microflown |
| Combination of two omnidirectional microphones virtual omnidirectional and figure of 8 microphone | Omni8 |
| Combination of two omnidirectional microphones, virtual back-to-back cardioid method | Back-to-back |
| Combination of two omnidirectional microphones, delay and sum method | DAS |
| Ambisonics | Soundfield |

Table 5.1: Abreviations of the methods used to generate a first-order microphone

## 5.1 Cardioid microphone

### 5.1.1 FRF

**Combination of two omnidirectional microphones**

Figure 5.1 shows the FRF of a virtual cardioid microphone generated using two omnidirectional microphones with a separation of 23.39 mm.
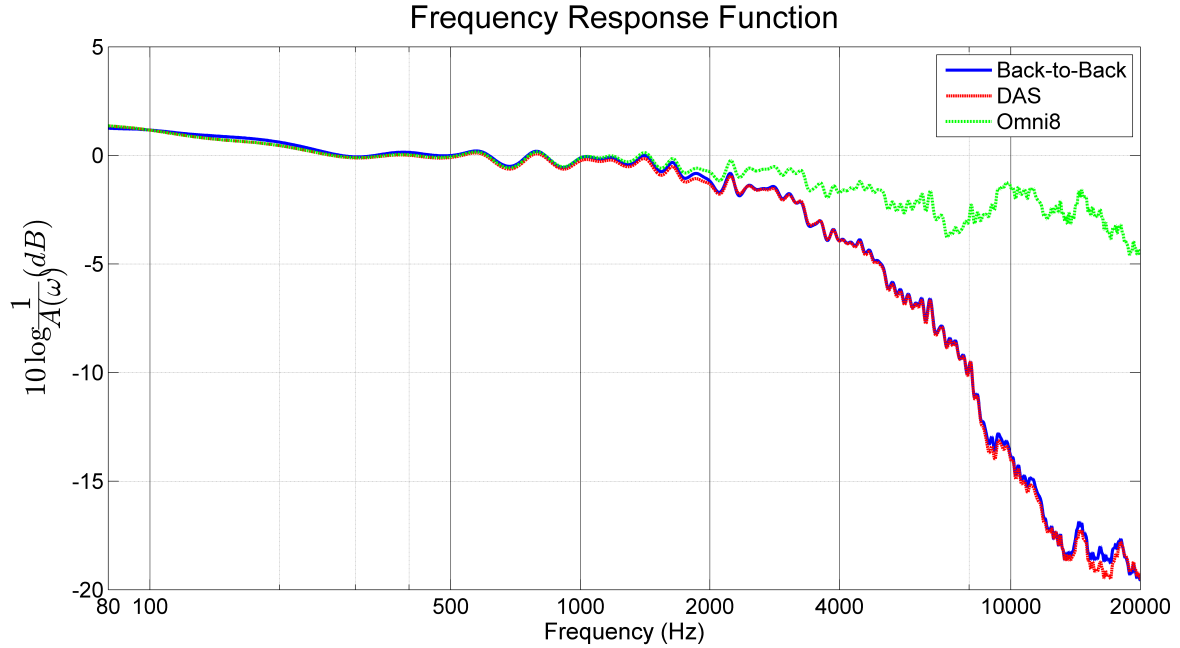
Figure 5.1: Virtual cardioid microphone's FRF with L=23.49 mm

Many of the trends that can be observed in Fig. 5.1 appear regardless of the microphone separation:

- For all the methods, from 80 Hz to a certain frequency $f_1$ the sensitivity of the virtual cardioid microphone decays with the frequency. Table 5.2 shows the values of $f_1$ and the first column of Table 5.3 shows the sensitivity decrease ratio for the different microphone separations L.

- For all the methods, from the frequency $f_1$ to the frequency $f_2$ the FRF is flat with oscillations of $\pm 1$ dB. Table 5.2 shows the values of $f_2$ for the different microphone separations L.

- For the methods DAS and back-to-back, from the frequency $f_2$ to the frequency $f_3$ shown in Table 5.2 the FRF decays with the frequency at the ratio indicated in the second column of Table 5.3. From the frequency $f_3$ to 20 kHz the FRF decays -6dB/oct for all the distances except L=10.44 mm in which the FRF remains constant within $\pm 2$ dB.

- The method omni8 from $f_2$ to 20 kHz presents a flat response with $\pm 3$ dB variations for all the distances.

| L (mm) | $f_1$ | $f_2$ | $f_3$ |
|---|---|---|---|
| 10.44 mm | 300 | 6000 | 12000 |
| 23.49 mm | 300 | 2000 | 4000 |
| 48.34 mm | 300 | 1000 | 2000 |
| 98.35 mm | 300 | 700 | 1000 |

Table 5.2: Virtual cardioid microphone FRF critical frequencies

| L (mm) | $1^{st}$ Slope | $2^{nd}$ Slope |
|---|---|---|
| 10.44 mm | -15 dB/oct | -6 dB/oct |
| 23.49 mm | -0.5 dB/oct | -4 dB/oct |
| 48.34 mm | -0.5 dB/oct | -3 dB/oct |
| 98.35 mm | -0.3 dB/oct | -6 dB/oct |

Table 5.3: Virtual cardioid microphone FRF parameters

As a summary of what has been discussed in this section, Figure 5.2 describes in a graphical manner the typical shape of the FRF function for all the distances and methods.
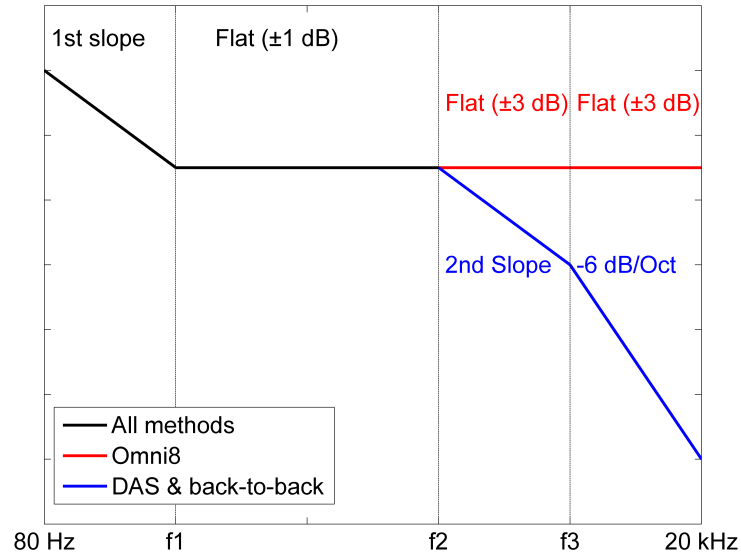


Figure 5.2: Standard behaviour of the FRF function for all the distances and methods when a cardioid microphone is generated

## Cardioid capsule, AVS-Microflown and Soundfield methods

Figure 5.3 shows the FRF of a cardioid capsule, a virtual cardioid generated from an acoustic vector sensor and a soundfield microphone.

37
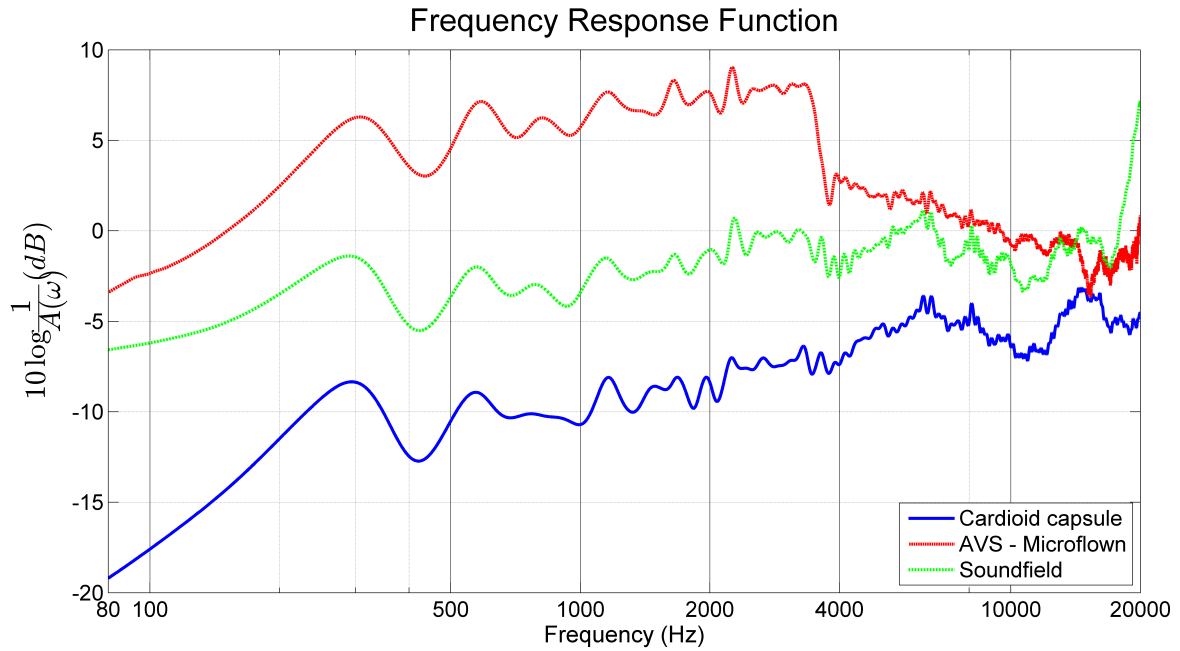
Figure 5.3: FRF of a cardioid capsule, a virtual cardioid generated from an acoustic vector sensor and a virtual cardioid generated using a soundfield microphone

- For all the methods the FRF at frequencies under 300 Hz decays critically and their use it is not recommended for this range.

- The FRF of the cardioid capsule tends to increase at approximately 2 dB/octave with ±2 dB variations from 300 Hz to 20 kHz.

- The virtual cardioid microphone generated with the AVS-Microflown method presents a FRF that increases 1 dB/octave from 300 Hz to approximately 3500 Hz with oscilations of ±2 dB. Between 3500 Hz and 4000 Hz the FRF decays 5 dB and after this drastic decay it decreases from 4 kHz to 20 kHz at 2 dB/octave.

- The FRF of the virtual cardioid created with the Soundfield Microphone increases 1 dB/octave from 300 Hz to 6 kHz suffering variations of ±2 dB. From 6 kHz to 18 kHz the FRF can be considered flat but it keeps the mentioned variations. Between 18 kHz and 20 kHz there is a drastic increase of sensitivity.

## 5.1.2   SNR

**Combination of two omnidirectional microphones**

Figure 5.4 shows the SNR from a virtual cardioid microphone generated using two omnidirectional microphones with a separation of 23.39 mm.
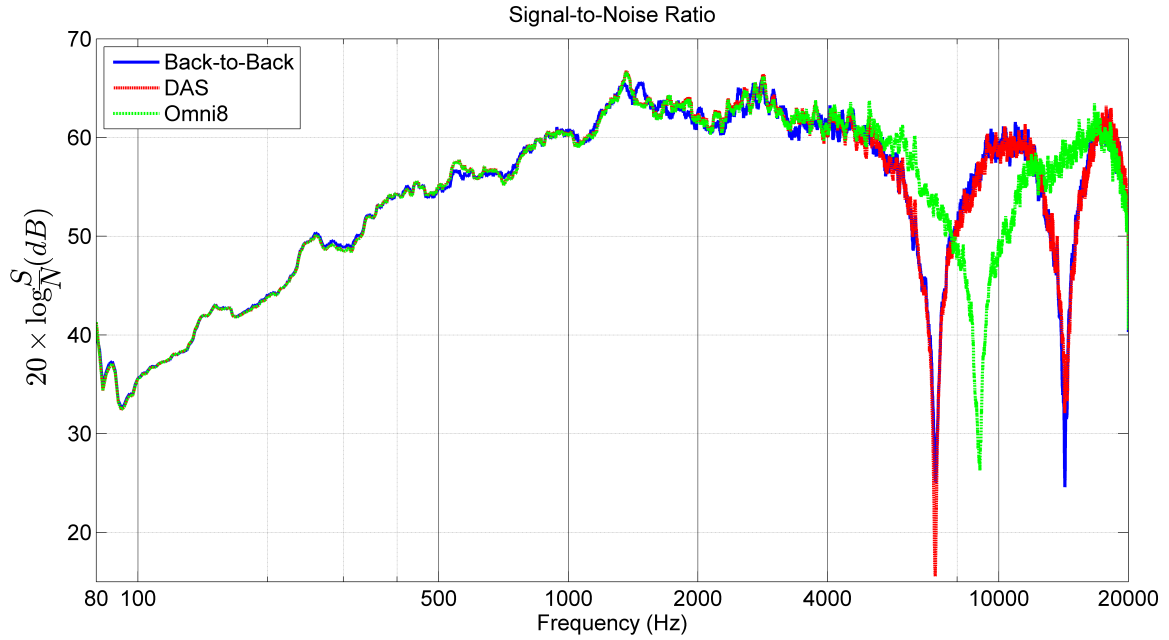
Figure 5.4: Virtual omnidirectional microphone's FRF with L=23.49mm

Many of the trends that can be observed in Fig. 5.4 appear regardless of the microphone separation:

- For all the methods, from 80 Hz to a certain frequency $f_1$ (shown in Table 5.4) the SNR fluctuates around the value shown in the first column of Table 5.5.

- From $f_1$ to the frequency $f_2$ shown in Table 5.4 the SNR increases with the frequency at the ratio shown in the second column of Table 5.5.

- From $f_2$ to 20 kHz the SNR can be considered to have the constant value shown in the third column of Table 5.5 with drop-offs of SNR at specific frequencies. For the methods DAS and back-to-back the minimums are located at the same frequencies.

| L (mm) | $f_1$ | $f_2$ |
|---|---|---|
| 10.44 mm | 500 | 2500 |
| 23.49 mm | 150 | 1000 |
| 48.34 mm | 100 | 500 |
| 98.35 mm | 100 | 300 |

Table 5.4: Virtual cardioid microphone SNR critical frequencies

| L (mm) | Initial value | Slope | Final value |
|---|---|---|---|
| 10.44 mm | 45 dB | +2 dB/oct | 58 dB |
| 23.49 mm | 35 | +4.5 dB/oct | 60 dB |
| 48.34 mm | 40 | +4 dB/oct | 60 dB |
| 98.35 mm | 45 | +3.5 dB/oct | 61 dB |

Table 5.5: Virtual cardioid microphone SNR parameters

## Cardioid capsule, AVS-Microflown and Soundfield methods

Figure 5.5 shows the SNR of a cardioid capsule and a virtual cardioid generated from an acoustic vector sensor and using a soundfield microphone.
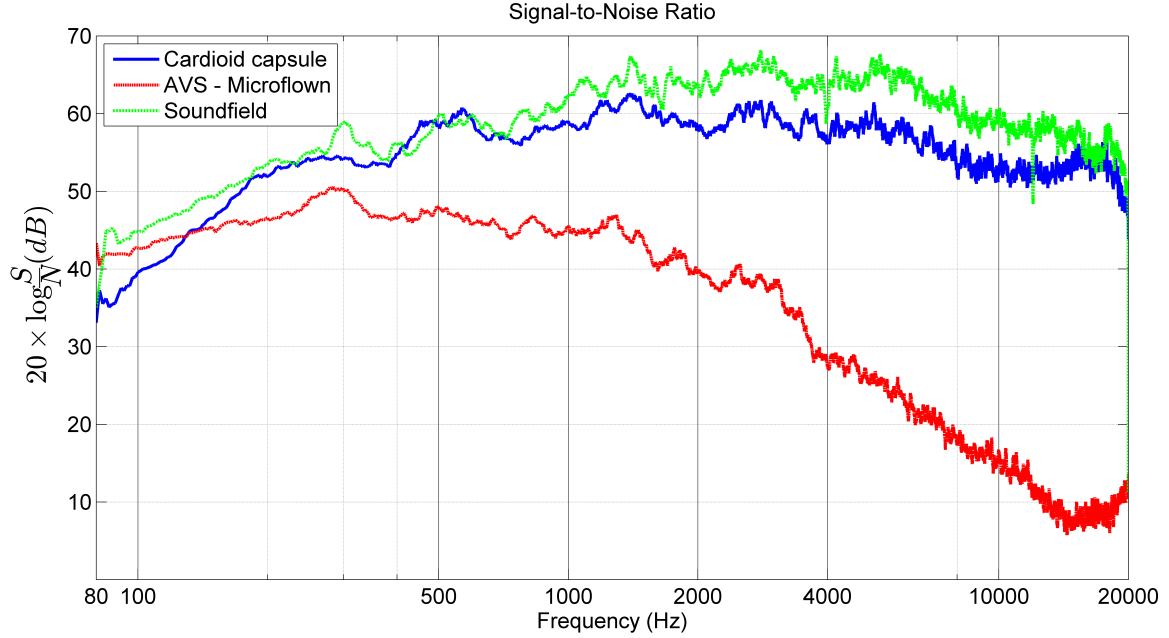


Figure 5.5: SNR of a cardioid capsule, a virtual cardioid generated from an acoustic vector sensor and a virtual cardioid generated using a soundfield microphone

- The signal to noise ratio of the cardioid capsule is greater than 30 dB in all the frequency range. The minimum value is located at low frequencies (35 dB) and it increases until 500 Hz, where the value keeps constant between 55 and 60 dB with some oscillations.

- A low SNR is the disadvantage of the AVS-Microflown method. Although the SNR is greater than 40 dB for the range 80 Hz to 2 kHz, afterwards the level of SNR decreases constantly until the minimum of 8 dB is reached at 15 kHz.

- The SNR of the soundfield method varies from 40 dB at low frequencies to 65 dB at mid and mid-high frequencies. For frequencies greater than 5 kHz the SNR decays slightly and the value at 20 kHz is around 50 dB.

### 5.1.3 Directivity error

**Combination of two omnidirectional microphones**

Figure 5.6 shows the directivity error of a virtual cardioid microphone generated using two omnidirectional microphones as a function of the distance. The blue, green and red curves represent the evolution of the directivity error at low, mid and high frequencies and different markers are used to differenciate between the back-to-back, DAS and omni8 methods. The colors of the background represent the different levels of directivity error defined in Table 4.3.
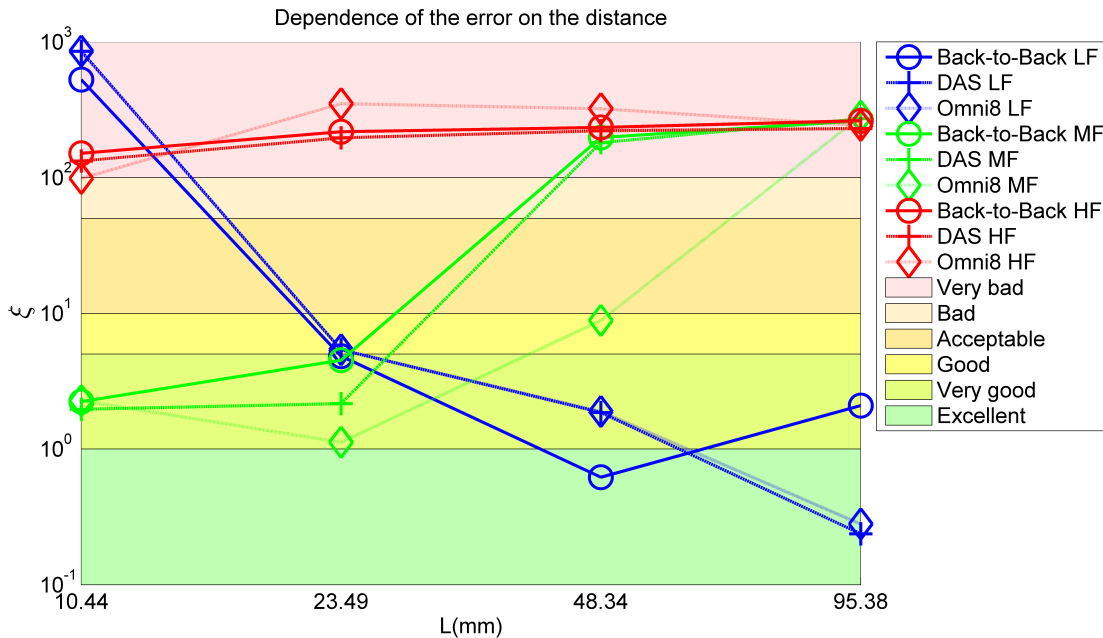


Figure 5.6: Directivity error of a virtual cardioid microphone as a function of the distance

In terms of the directivity error all the methods used to combine two omnidirectional microphones (back-to-back, DAS and Omni8) present similar results. The important variable to take into account is the distance L between the two omnidirectional microphones. As can be seen in Fig. 5.6 the distance determines the accuracy of the generated virtual pattern:

- For low frequencies it is better to have a greater separation between the microphones. The error obtained for L=95.38 mm is less than 1 in the cases of DAS and Omni8

methods, which means that the virtual pattern has an "excellent" fit to the ideal pattern. The back-to-back presents "very good" results of directivity error at low frequencies.

- The error at mid frequencies has its lower directivity error at medium distances such as L=23.49. Using this distance all the methods present a "very good" value of error $(0 < \xi < 1)$.

- The drawback of these methods is at high frequencies. In all the cases the obtained error is "very bad" for the separations tested in this study. Although, it is important to note that the frequency range specified by the manufacturer for the G.R.A.S microphones is limited at 10 kHz.

As can be observed in Figure 5.6, non of the tested distances are adequate at high frequencies in terms of the directivity error. At mid frequencies the best option is a separation L=23.49 mm between the microphones and at low frequencies the best option is the largest separation L=95.38 mm between microphones. Regarding to the methods, the omni8 method offers the optimum results at low and mid frequencies and the DAS method offers also an "excellent" value of error at low frequencies.

**Cardioid capsule, AVS-Microflown and Soundfield methods**

Figure 5.7 shows the directivity error of a cardioid capsule, a virtual cardioid generated from an acoustic vector sensor and using a soundfield microphone. The blue, green and red curves represent the evolution of the directivity error at low, mid and high frequencies depending on the evaluated method. The colors of the background represent the different levels of directivity error defined in Table 4.3.
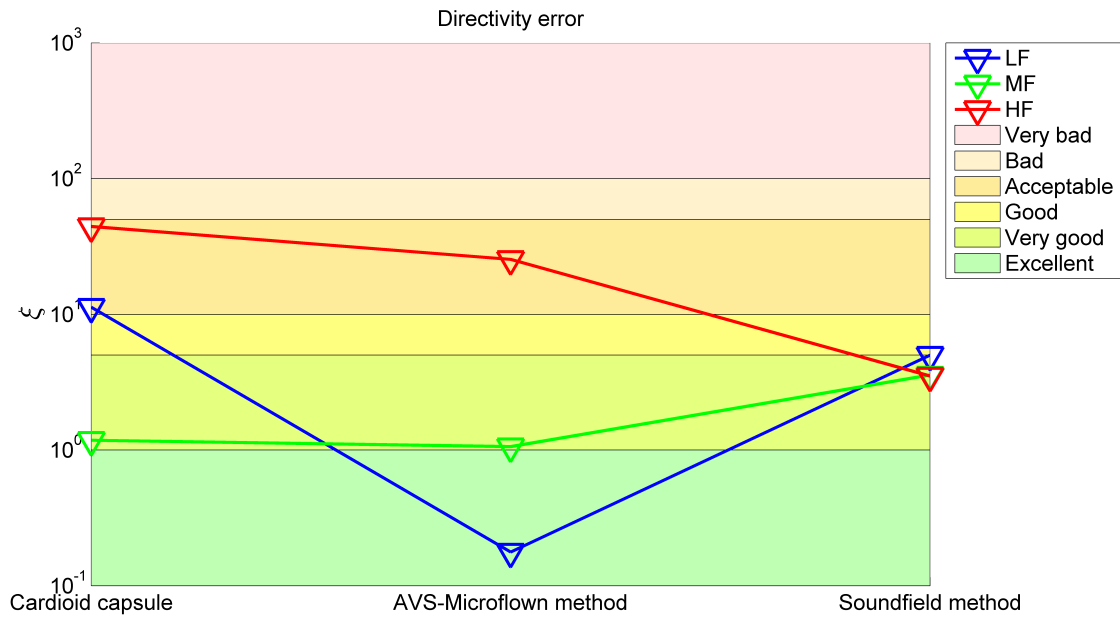
Figure 5.7: Directivity error of a cardioid microphone generated with a cardioid capsule, AVS-Microflown method and Soundfield methods

- The analyzed cardioid capsule offers a "acceptable" fit at low frequencies. At mid frequencies the directivity error is "very good" and at high frequencies the fit is at the border between "acceptable" and "bad".

- The directivity error of the AVS-Microflown method presents "excellent" fit at low a directivity error of $\xi \leq 1$. At mid frequencies the error is "very good" and at high frequencies the error increases drastically due to the low SNR from 10 to 20 kHz (SNR $<$ 15 dB).

- The directivity error of the soundfield microphone offers a "good" fit in all the frequencies analyzed.

The soundfield microphone is the optimum solution since it offers a good fit in all the ranges. Looking only into low and mid frequencies the best method is the AVS-Microflown, since it can provide an "excellent" and a "very good" fit at low and medim frequencies respectively.

## 5.2   Figure of 8 microphone

### 5.2.1   FRF

**Combination of two omnidirectional microphones**

Figure 5.8 shows the FRF of a virtual figure of 8 microphone generated using two omni-directional microphones with a separation of 23.39 mm.
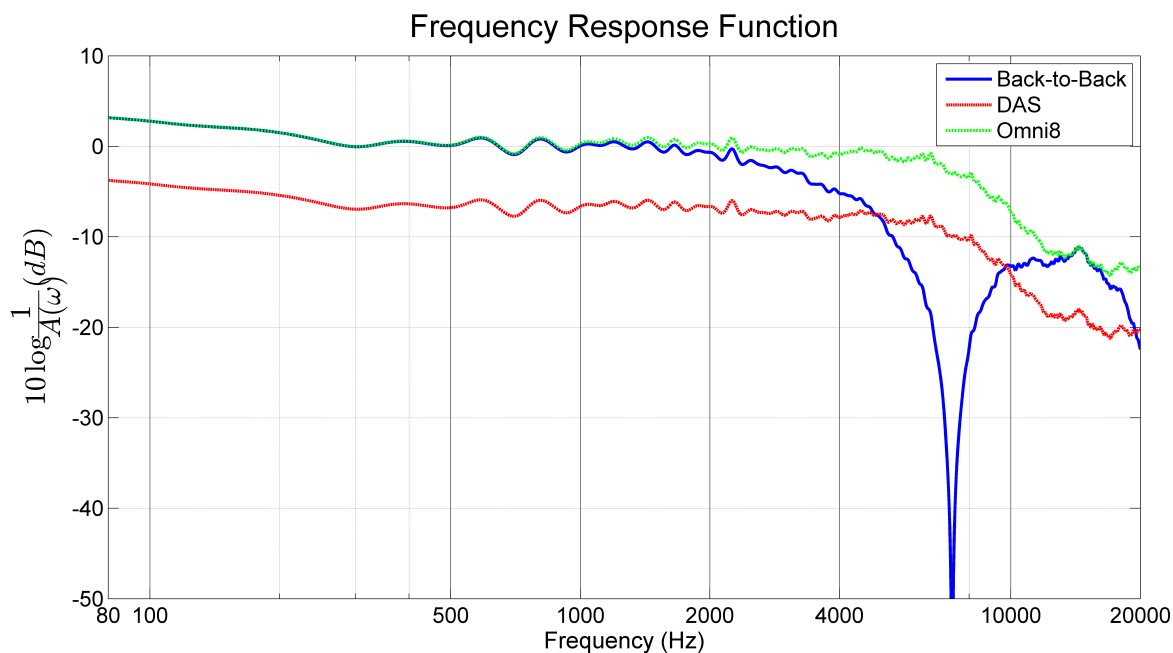


Figure 5.8: Virtual omnidirectional microphone's FRF with L=23.49 mm

Many of the trends that can be observed in Fig. 5.8 appear regardless of the microphone separation:

- For all the methods, from 80 Hz to the frequency $f_1$ shown in Table 5.6 the sensitivity of the virtual cardioid microphone decays with the frequency at the ratio shown in the first column of Table 5.7.

- For all the methods, from $f_1$ to the frequency $f_2$ shown in Table 5.6 the FRF is flat with oscillations within the range shown in the second column of Table 5.7.

- For the methods DAS and omni8, from $f_2$ to the frequency $f_3$ shown in Table 5.6 the FRF decays with the frequency at the ratio shown in the third column of Table 5.7.

- From $f_3$ to 20 kHz the FRF presents small variations around of the value shown in the fourth column of Table 5.7. The method back-to-back presents a similar tendency at this range of frequencies with drop-offs of sensitivity at specific frequencies.

- The FRF of the methods DAS and omni8 is the same with a difference of sensitivity of 4 dB.

| L (mm) | $f_1$ | $f_2$ | $f_3$ |
|---|---|---|---|
| 10.44 mm | 300 | 8000 | 11000 |
| 23.49 mm | 300 | 7000 | 12000 |
| 48.34 mm | 300 | 2000 | 5000 |
| 98.35 mm | 300 | 1000 | 4000 |

Table 5.6: Virtual figure of 8 microphone parameters

| L (mm) | $1^{st}$ Slope | Oscillations | $2^{rd}$ Slope | $3^{th}$ Slope |
|---|---|---|---|---|
| 10.44 mm | -18 dB/oct | ±1 dB | -5 dB/oct | -3 dB/oct |
| 23.49 mm | -1 dB/oct | ±0.5 dB | -6 dB/oct | flat(±1 dB) |
| 48.34 mm | -1 dB/oct | ±1 dB | -3.5 dB/oct | -9 dB/oct |
| 98.35 mm | -0.5 dB/oct | ±1 dB | -3.5 dB/oct | -7.5 dB/oct |

Table 5.7: Virtual figure of 8 microphone critical frequencies

As a summary of what has been discussed in this section, Figure 5.9 describes in a graphical manner the typical shape of the FRF function for all the distances and methods.
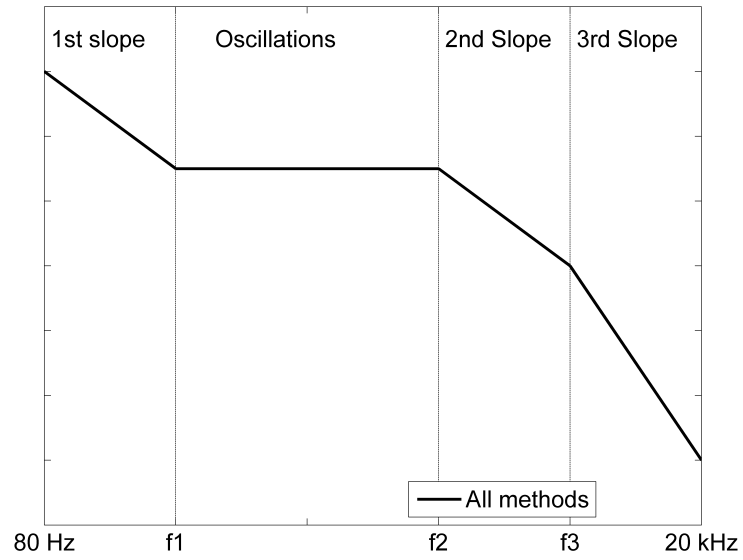
Figure 5.9: Standard behaviour of the FRF function for all the distances and methods when a figure of 8 microphone is generated

**AVS-Microflown and Soundfield methods**

Figure 5.10 shows the FRF of figure of 8 microphone generated from an acoustic vector sensor and using a soundfield microphone.
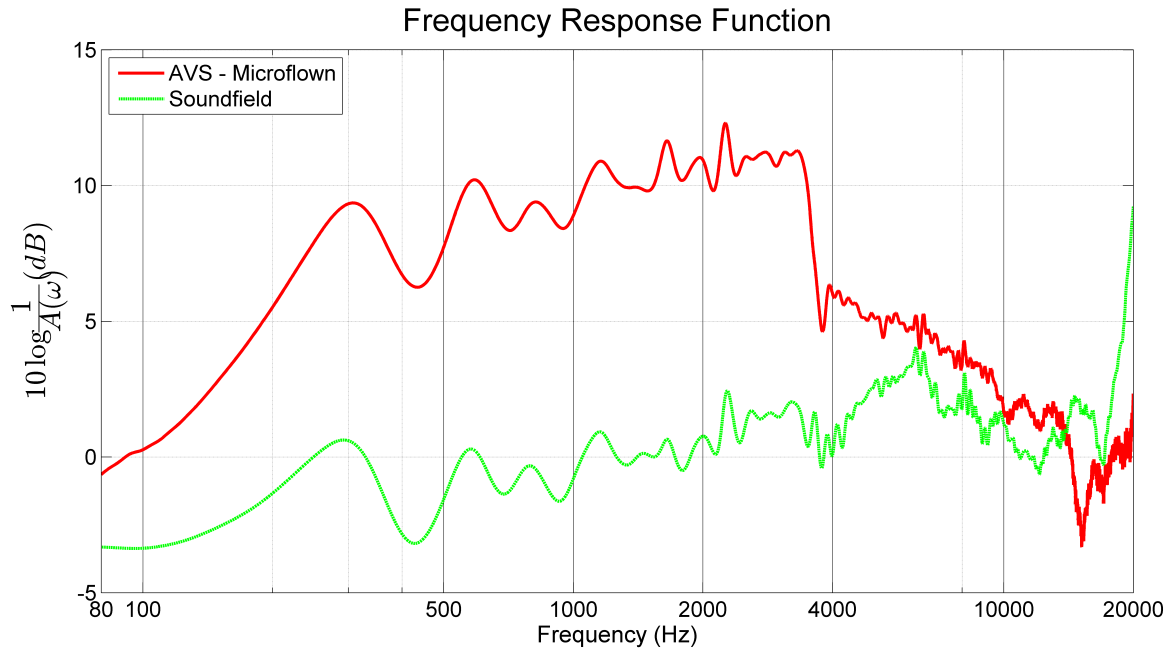
Figure 5.10: FRF of a figure of 8 microphone generated with AVS-Microflown and Sound-field methods

- For both methods the FRF at frequencies less than 300 Hz decays critically and their use it is not recommended at this range.

- The figure of 8 provided by the vector sensor presents a FRF which increases 1.5 dB/octave from 300 Hz to approximately 3500 Hz and suffers oscilations of ±3 dB. Between 3500 Hz and 4000 Hz the FRF decays 5 dB and after this drastic decay it decreases from 4 kHz to 20 kHz at 2 dB/octave presenting another minimum of sensitivity at 15 kHz.

- The FRF of the virtual cardioid created with the Soundfield Microphone presents an increase of 1.7 dB/octave within 300 Hz and 6kHz, with fluctiatons of ±2 dB around this main tendency. Within the range from 6 kHz to 20 kHz the FRF can be considered flat but it conserves the mentioned variations. Between 18 kHz and 20 kHz there is a drastic increase of sensitivity.

## 5.2.2   SNR

**Combination of two omnidirectional microphones**

Figure 5.11 shows the SNR of a virtual cardioid microphone generated using two omnidi-rectional microphones with a separation of 23.39 mm.
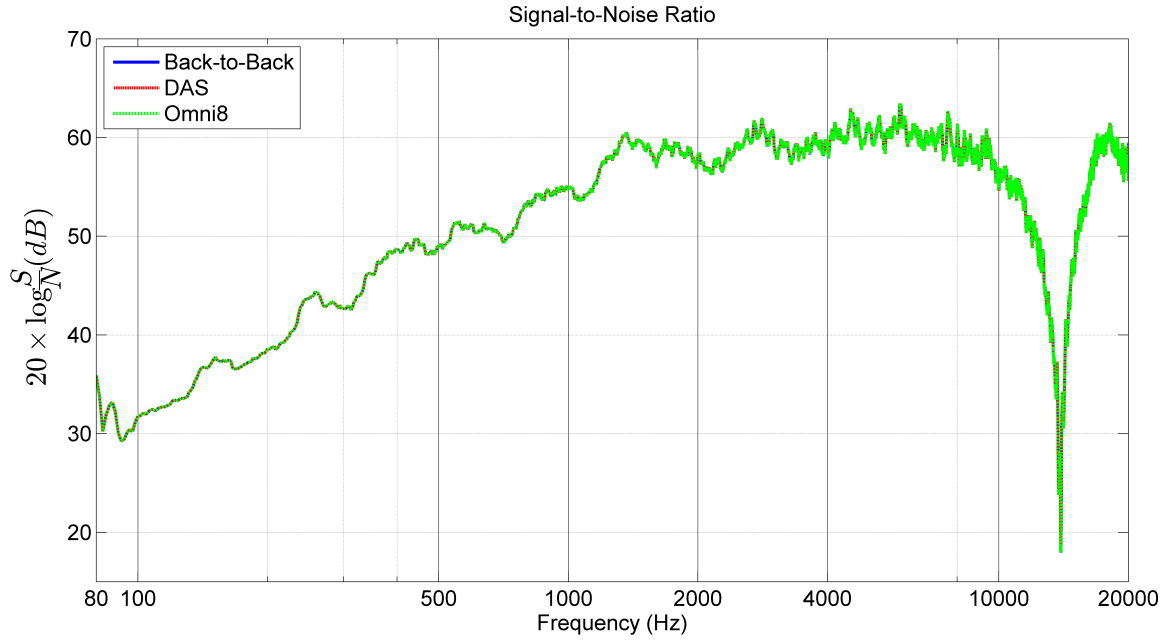
Figure 5.11: Virtual omnidirectional microphone's SNR with L=23.49 mm

Many of the trends that can be observed in Fig. 5.11 appear regardless of the microphone separation:

- The SNR of the virtual figure of 8 microphone is the same regardless of the method used.

- For all the methods, from 80 Hz to the requency $f_1$ shown in Table 5.8 the SNR fluctuates around the value given in the first column of Table 5.9.

- From $f_1$ to the frequency $f_2$ shown in Table 5.8 the SNR increases with the frequency at the rate indicated in the second column of Table 5.9.

- From $f_2$ to 20 kHz the level keeps constant around the value shown in the third column of Table 5.9 dB presenting drop-offs of SNR at specific frequencies.

| L (mm) | $f_1$ | $f_2$ |
|---|---|---|
| 10.44 mm | 300 | 2000 |
| 23.49 mm | 150 | 1300 |
| 48.34 mm | 150 | 1000 |
| 98.35 mm | 100 | 500 |

Table 5.8: Virtual cardioid microphone parameters

| L (mm) | Initial value | Slope | Final value |
|--------|--------------|-------|-------------|
| 10.44 mm | 40 dB | +2 dB/oct | 55 dB |
| 23.49 mm | 33 dB | +3.5 dB/oct | 59 dB |
| 48.34 mm | 37 dB | +3 dB/oct | 60 dB |
| 98.35 mm | 42 dB | +4 dB/oct | 60 dB |

Table 5.9: Virtual cardioid microphone parameters

**AVS-Microflown and Soundfield methods**

Figure 5.12 shows the SNR of a figure of 8 microphone generated using an acoustic vector sensor and a soundfield microphone.
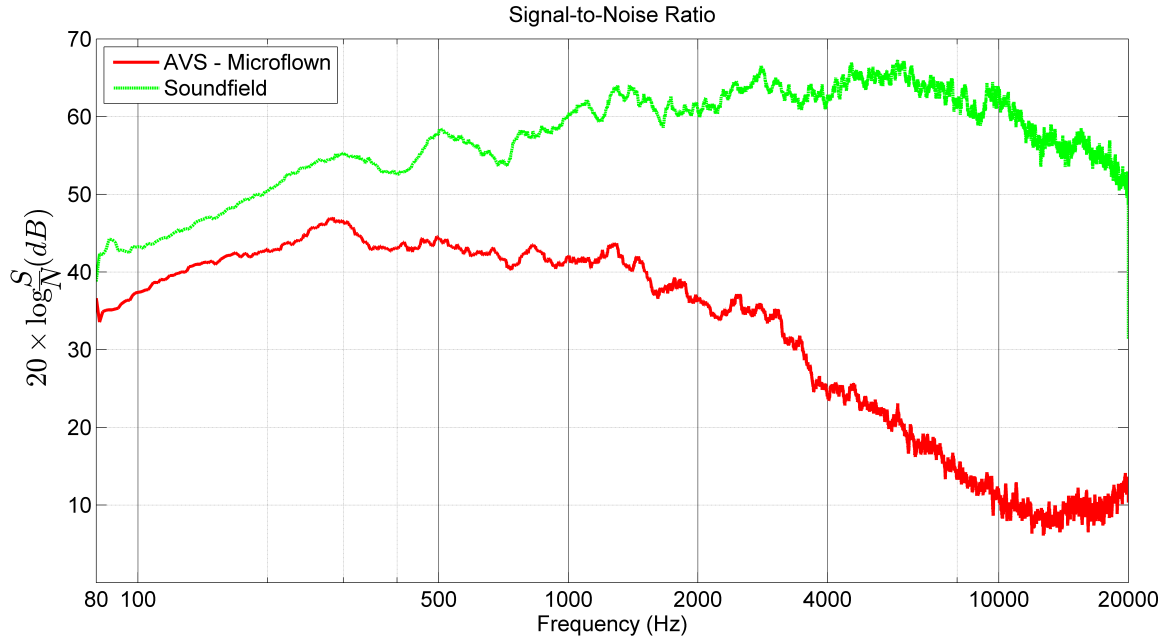


Figure 5.12: SNR of a figure of 8 microphone generated with AVS-Microflown and Soundfield methods

- As in the cardioid case, when generating a figure of 8 microphone using the AVS-Microflown method the SNR presents some problems. The value of the SNR is greater than 35 dB for the range from 80 Hz to 2 kHz. After that the level of SNR decreases constantly until the minimum of 8 dB is reached around 13 kHz.

- The SNR of the soundfield method varies from 40 dB at low frequencies to 65 dB at mid and mid-high frequencies. For frequencies greater than 5 kHz the SNR decays slightly and the value at 20 kHz is around 50 dB.

### 5.2.3 Directivity error

**Combination of two omnidirectional microphones**

Figure 5.13 shows the directivity error of a virtual cardioid microphone generated using two omnidirectional microphones as a function of the distance. The blue, green and red curves represent the evolution of the directivity error at low, mid and high frequencies. The colors of the background represent the different levels of directivity error defined in Table 4.3.
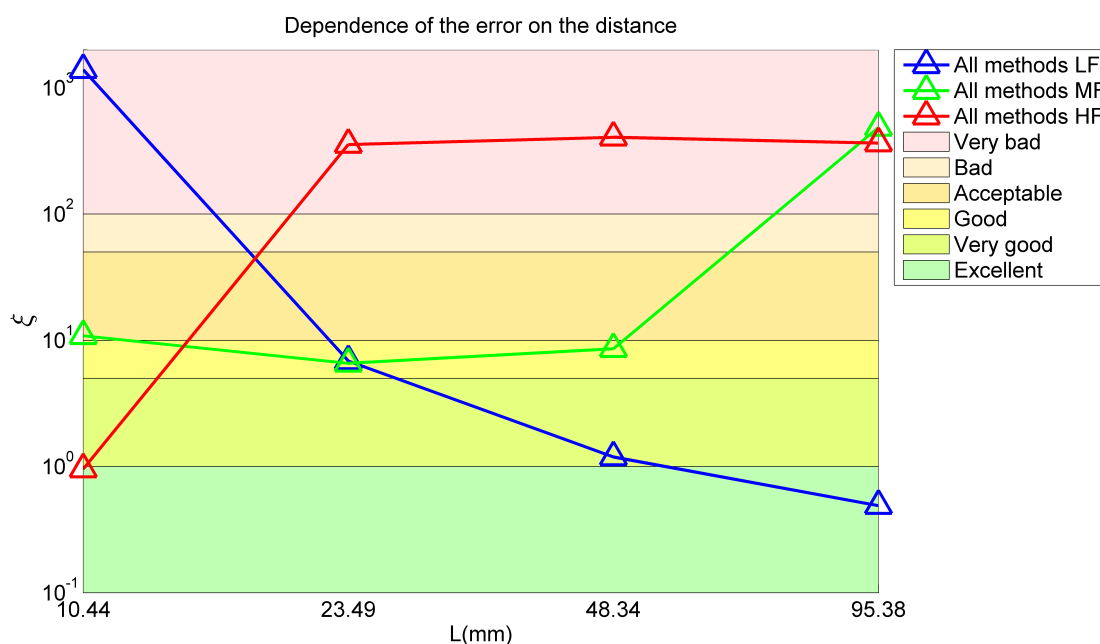


Figure 5.13: Directivity error of a virtual figure of 8 microphone as a function of the distance

As can be seen in Fig. 5.13 when generating a figure of 8 it is possible to achieve a low error for high frequencies as opposite to what happens when generating a cardioid.

In the present case the error is the same regardless of the method used to generate the virtual microphone. As in the case of a virtual cardioid, the error depends on the distance between the microphones:

- At low frequencies an "excellent" and "very good" values of error can be achieved if the distances are L=95.38 mm and L=48.23 mm respectively.

- At mid frequencies the medium distances (L=23.49 and L=48.34 mm) are appropriated to obtain a "good" value of error ($\xi \leq 10$).

- If the distance between the analyzed microphones is very small - i.e. L=10.44 mm - the value of the error at high frequencies is $\xi$=1, which means that the analyzed pattern fit can be qualified as "excellent".

As in the cardioid case, for a virtual figure of 8 microphone the best option at mid frequencies is a separation between microphones of L=23.49 mm and at low frequencies the best option is a big separation of L=95.38 mm. Unlike in the cardioid case, a small distance L=10.44 mm gives an "excellent" directivity error result. Regarding the different generation methods (back-to-back, DAS and omni8) the performance is the same in all the cases when generating a figure of 8 microphone.

### AVS-Microflown and Soundfield methods

Figure 5.14 shows the directivity error a figure of 8 microphone generated using a sound-field microphone. The blue, green and red curves represent the evolution of the directivity error at low, mid and high frequencies respectively as a function of the evaluated method. The colors of the background represent the different levels of directivity error defined in Table 4.3.
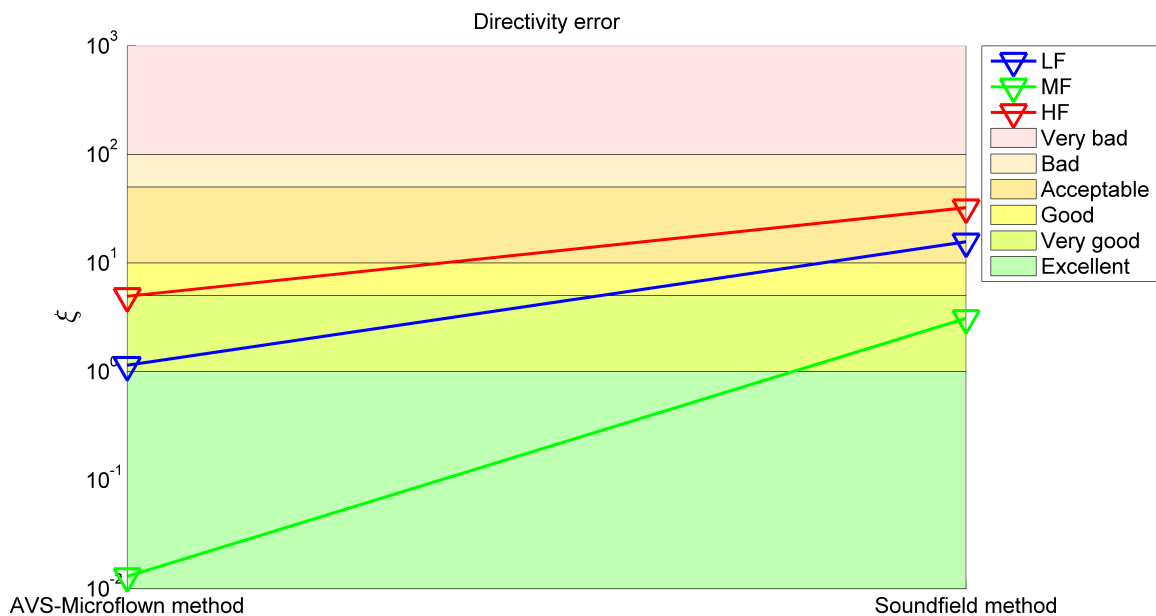


Figure 5.14: Directivity error of a figure of 8 microphone generated with AVS-Microflown and Soundfield methods

- The AVS-Microflown method is capable of provide "excellent" results of directivity error at low frequencies with errors of $\xi$ <1. At mid frequencies the value of the

51

directivity error is "very good". At high frequencies the value of the error is "good", but it is important to remember that the SNR is low ($\approx$ 15 dB).

- The soundfield microphone presents "very good" values of error at low frequencies, but at mid and high frequencies the error is only "acceptable".

In general, the AVS-microflown offers smaller directivity error at all the frequencies despite having a low SNR at high frequencies.

# Chapter 6

# Discussion

This Chapter contains an analysis of the results obtained from the experiments. Tables 6.1 and 6.2 summarize and compare the main characteristics of the analyzed methods divided into the frequency ranges. The best method and its main characteristics is discussed at every frequency range.

In the case of the combination of signals of two omnidirectional microphones, since this method has multiple post-processing techniques and distances between microphones. Tables 6.1 and 6.2 show only the characteristics of the best post-processing technique and distance at every different frequency range. Since the FRF and SNR are similar regardless of the post-processing technique used, the criterium used to choose the best method at every frequency range is based on selecting the technique and distance that generate the lowest directivity error.

**Cardioid directivity pattern**

| Method | FRF | Directivity Error | SNR |
|---|---|---|---|
| **Frequency range: 80 - 200 Hz** | | | |
| 2 omni (Omni8 & DAS, 95.38 mm) | -0.3 dB/oct | $\xi = 0.24$ (excellent) | >45 dB |
| Cardoid capsule | +6 dB/oct | $\xi = 11.2$ (acceptable) | >35 dB |
| AVS - Microflown | +5 dB/oct | $\xi = 0.18$ (excellent) | >40 dB |
| Soundfield | +3 dB/oct | $\xi = 5$ (good) | >35 dB |
| **Frequency range: 200 - 4000 Hz** | | | |
| 2 omni (Omni8, L=23.49 mm) | flat ($\pm 1$ dB) | $\xi = 1.1$ (very good) | >42 dB |
| Cardoid capsule | +2 dB/oct ($\pm$ 2 dB) | $\xi = 1.2$ (very good) | >51 dB |
| AVS - Microflown | +1 dB/oct($\pm$ 2 dB) | $\xi = 1.1$ (very good) | >29 dB |
| Soundfield | +1 dB/oct ($\pm$ 2 dB) | $\xi = 3.6$ (very good) | > 52 dB |
| **Frequency range: 4000 - 20000 Hz** | | | |
| 2 omni (Omni8, L=10.44 mm) | flat ($\pm 2.5$ dB) | $\xi = 98.5$ (bad) | >40 dB |
| Cardoid capsule | +2 dB/oct ($\pm 2$ dB) | $\xi = 44.3$ (acceptable) | >48 dB |
| AVS - Microflown | -2 dB/oct ($\pm 1$ dB) | $\xi = 25.4$ (acceptable) | >8 dB |
| Soundfield | flat ($\pm 6$ dB) | $\xi = 3.5$ (very good) | >50 dB |

Table 6.1: Comparison of the performance offered by the different methods at different frequency ranges when a cardioid microphone is generated

The results included in Table 6.1 lead to the following conclusions:

- At low frequencies the optimum method to generate a cardioid microphone consists of two omnidirectional microphones with separation L=95.38 mm with the DAS or the Omni8 processing algorithm. The SNR, FRF and directivity error of this method are the best of the studied methods at this frequency range.

- At mid frequencies all the methods included in Table 6.1 present a "very good" value of directivity error but the most balanced method is the Omni8, since the frequency response is flat at this range and the value of SNR is considerably high.

- At high frequencies the only suitable method is the soundfield microphone. This method presents a "very good" value of directivity error, a flat response (altough it presents considerably big variations) and a value of SNR over 50 dB.

- Looking into the frequency range of interest for the application of the project SOUNDTRACK (low and mid frequencies) the optimum method is to combine the signals of two omnidirectional microphones. At low frequencies the distance between microphones should be L=95.38 mm and best the post-processing algorithms are DAS or Omni8, while at mid frequencies the best distance is L=23.49 mm and Omni8 is the best processing algorithm. Therefore, with an array of three matched microphones the entire low and mid frequency range could be covered.

54

**Figure of 8 directivity pattern**

| Method | FRF | Directivity Error | SNR |
|---|---|---|---|
| **Frequency range: 80 - 200 Hz** | | | |
| 2 omni (all methods, 95.38 mm) | -1 dB/oct | $\xi = 0.49$ (excellent) | >39 dB |
| AVS - Microflown | +5 dB/oct | $\xi = 1.2$ (very good) | >34 dB |
| Soundfield | +1.5 dB/oct | $\xi = 15.7$ (acceptable) | >40 dB |
| **Frequency range: 200 - 4000 Hz** | | | |
| 2 omni (all methods, 23.49 mm) | flat ($\pm 0.5$ dB) | $\xi = 6.57$ (good) | >53 dB |
| AVS - Microflown | +1.5 dB/oct ($\pm 2$ dB) | $\xi = 0.01$ (excellent) | >25 dB |
| Soundfield | +1.7 dB/oct ($\pm 1.5$ dB) | $\xi = 3.1$ (very good) | > 50 dB |
| **Frequency range: 4000 - 20000 Hz** | | | |
| 2 omni (L=10.44 mm) | -2 dB/oct ($\pm 0.5$ dB) | $\xi = 0.95$ (excellent) | >50 dB |
| AVS - Microflown | -2 dB/oct ($\pm 3$ dB) | $\xi = 4.9$ (very good) | >8 dB |
| Soundfield | flat ($\pm 3$ dB) | $\xi = 32.3$ (acceptable) | >50 dB |

Table 6.2: Comparison of the performance offered by the different methods at different frequency ranges when a figure of 8 microphone is generated

The results included in Table 6.2 lead to the following conclusions:

- At low frequencies the best option to generate a figure of 8 microphone consists of two omnidirectional microphones with a separation L=95.38 mm. The FRF variations (-1 dB/oct) and directivity error ("excellent") presented by this method are the best at this frequency range. Moreover, the SNR value (39 dB) is very similar to the best value of SNR at this range (40 dB).

- At mid frequencies all the methods present good results in some of the analyzed parameters. In terms of FRF and SNR the combination of signals of two omnidirectional microphones with L=23.49 mm is the best option at this range. In terms of directivity error the AVS-Microflown error presents "excellent" results. The Soundfield microphone presents good results in SNR and directivity error. The most balanced method at this range is the combination of two omnidirectional microphones due to the flat FRF, "good" value of error and high value of SNR.

- At high frequencies the only suitable method is the combination of two omnidirectional microphones with a distance L=10.44 mm. The FRF decays 8 dB/octave but this decayment could be corrected using a high-pass filter, and the values of directivity error and SNR are the best of the analyzed methods. Although the AVS-Microflown presents "very good" values of error, the SNR is only 8 dB and this is not appropriate for measurement purposes.

- The optimum method suitable for all the frequencies is the combination of two omnidirectional microphones. Since the results are the same for all the post-processing

techniques when a figure of 8 is generated, all the studied techniques (Omni8, back-to-back and DAS) are appropriated. This is the only method that presents "good" or "excellent" results of directivity error with a suitable value of SNR. The FRF presents some variations that could be corrected using a filter at high frequencies. It is important to note that the optimum distance between the microphones is different at every frequency range - L=95.38 mm, L=23.49 mm and L=10.44 mm for low, mid and high distances respectively - and in practical terms the realization of this method would require at least 4 omnidirectional microphones in order to cover the three frequency ranges or at least 3 microphones to cover the range of interest (low and mid frequencies).

# Chapter 7

# Conclusions

## 7.1 Technical conclusions

In this master thesis four different methods to generate a first-order directional microphone have been experimentally tested and compared. The four methods compared are a cardioid capsule and a virtual first-order microphone generated using an array of two omnidirectional microphones, an acoustic vector sensor and a Soundfield microphone.

The studied characteristics of the first-order microphone generated with each method are the frequency response (FRF), the signal-to-noise ratio (SNR) and the directivity error. These characteristics have been studied separatelly for low frequencies within 80 Hz and 200 Hz, mid frequencies within 200 Hz and 4 kHz, and high frequencies within 4 kHz and 20 kHz.

Since there is an infinite number of possible first-order directivity parameters, in this thesis only cardioid and figure of 8 directivity patterns have been studied.

Regarding the virtual first-order microphone generated using an array of two omnidirectional microphones the results show that the distance between the two microphones determines the frequency range of the virtual microphone. To obtain a flat frequency response, a high signal-to-noise ratio and a low directivity error at low frequencies a distance of 95.38 mm is the best among those tested. For mid frequencies the best distance is 23.39 mm, and for high frequencies a distance of 10.44 mm is the best in the case of a figure of 8 directivity while in the case of cardioid directivity non of the separations studied provided satisfactory results.

Three different signal processing algorithms have been studied for the case of the virtual first-order microphone generated using an array of two omnidirectional microphones. The method Omni8 generates a virtual first-order microphones combining the signals of a virtual omnidirectional and a virtual figure of 8 microphone created using the signals of two omnidirectional microphones. The method DAS consists of the combination of a signal from an omnidirectional microphone with a phase shifted delayed signal from another omnidirectional microphone. Finally, the back-to-back method combines the signals of two virtual cardioid microphones with inverted patterns created using the signals of two omnidirectional microphones. They all present very similar results but the main

difference between the methods is the directivity error at specific frequency ranges and distances between microphones. The algorithm based on the combination of a virtual omnidirectional and figure of eight microphones presented the best results considering both directivity patterns and the different frequency ranges.

Comparing the different methods, at low frequencies the virtual first-order microphone generated using an array of two omnidirectional microphones is the only method that provided satisfactory results. In this range the acoustic vector sensor and the soundfield microphone present a very low sensitivity at low frequencies and therefore non of them is suitable in this range.

At mid frequencies the virtual first-order microphone generated using an array of two omnidirectional microphones is the preferred method because of a flat FRF a high SNR. However, the performance of the Soundfield microphone, the acoustic vector sensor and the cardioid capsule is also good in this range.

At high frequencies the virtual first-order microphone generated using an array of two omnidirectional microphones is the best choice for a figure of 8 directivity pattern, while the sound field microphone is the best option for a cardioid directivity pattern. The performace of the acoustic vector sensor is limited in this frequency range by a very low SNR and the cardioid capsule presents a high directivity error.

To sum up, the results show that to generate both a cardioid microphone and a figure of 8 microphone the best choice is to an array of two omnidirectional microphones. In the case of a cardioid microphone it is possible to build a virtual cardioid microphone suitable for the low and mid frequency ranges using an array of 3 microphones. Moreover, in the case of a figure of 8 directivity, by adding a fourth microphone to the array, the range covered could extend up to high frequencies.

## 7.2   Project applications

The conclusions extracted from this thesis have a direct impact on the aircraft noise monitoring terminal (NMT) designed in the SOUNDTRACK project. As a result of this thesis, this NMT incorporates four arrays of two omnidirectional microphones located at the vertices of a regular tethraedron in order to generate 4 virtual first-order directional microphones. This microphones are used to locate the direction of arrival of the sound produced by the aircraft at low frequencies removing the influence of the ground reflections and other ground borne sources. In addition, one of these arrays includes a third microphone allowing to create a virtual first-order microphone to monitor the aircraft noise within the whole range between 200 Hz and 4 kHz.

Besides the main application, specific parts of this project could be used for research or educational purposes:

- The files resulting from the acoustic measurements could be used for characterizing the performance of the test sensors analyzed in this document.

- The developed functions could be used to generate virtual first-order microphones using different models of test sensors.

- The final results presented in this thesis represent an improvement of the understanding of the performance of the different methods in general.

## 7.3   Further work

If the problem studied in this project is object of future work, it could be complemented by the realization of a theoretical model that generates the FRF, SNR and directivity of the first-order directional microphones generated with the different methods using the data of FRF, SNR and directivity of the individual test sensors. This theoretical model could be useful to perform an analysis of the performance of the different methods regardless of the sensors used in the measurements.

Performing the same experiments using a number of different cardioid capsule would present different results and therefore would give a better idea of the general behaviour of cardioid capsules of different qualities.

# Bibliography

[1] I. J. Tashev, "Sound Capture and Processing: Practical Approaches", Wiley, Hoboken, New Jersey (2009).

[2] C. Faller, "Signal Processing for Audio and Acoustics", EPFL Lausanne, Switzerland (2013).

[3] H. F. Olson, *Gradient Microphones*, Journal of Acoustics Society of America Vol 17, pp. 192-198 (1945).

[4] G.W. Elko and A.N Pong "A steerable and variable first-order differential microphone array" Acoustics, Speech, and Signal Processing, IEEE International Conference on. **1**, (1997).

[5] P. Sjösten, *Microphones Continued*, Part 2. Chapter 5, Chalmers University, Sweeden, 2012.

[6] P. Svensson, *Audio Technology Lecture Notes*, Norwegian University of Science and Technology, Trondheim, Norway, 2013.

[7] G.W. Elko and A.N Pong, "A Simple Adaptive First-Order Differential Microphone", Applications of Signal Processing to Audio and Acoustics, IEEE ASSP Workshop (1995)

[8] K. Farrar, "Soundfield Microphone", Wireless World, pp. 48-50 (1979)

[9] Morset Sound Development, "Loadimp Function", Trondheim, Norway (1998-2003).

# Annex A

# Used equipment technical data

| Model | Type | Serial Number | Usage | Official Datasheet |
|---|---|---|---|---|
| Genelec 1029A | 2-way active speaker | SINTEF BA-2042 | All methods | Genelec website |
| Norsonic nor265 | Turntable | 29300 | All methods | Norsonic website |
| LynxTWO-C | PCI 6-input 2-output soundcard | —— | All methods | Lynx website |
| AKG C460B | Cardioid microphone system | —— | Method 3.1 | AKG website |
| Shure FP23 | Preamplifier | 00967 | Method 3.1 | Shure website |
| Microflown USP probe | 1 Pressure & 3 velocity sensors | UR-900843 | Method 3.2 | Microflown website |
| Microflown MFSC-4 | 4-channel signal conditioner | SC4-900843 | Method 3.2 | Microflown website |
| G.R.A.S. 40AI | Paired omnidirectional capsules | 119022/119047 | Method 3.3 | G.R.A.S. website |
| Norsonic nor1201 | Microphone preamplifiers | 23824/30651 | Method 3.3 | Norsonic website |
| Norsonic nor336 | 2-channel signal amplifier | 20579 | Method 3.3 | G&A website |
| TSL Soundfield SPS422B | Ambisonics Microphone | C597 | Method 3.4 | TSL website |
| TSL Soundfield SPS422B | Ambisonics Signal Processor | 00715 | Method 3.4 | TSL website |

Table A.1: Used equipment technical data

# Annex B

# Matlab developed functions

## B.1   Virtual Microphone Code

### B.1.1   Description

The goal of this function is to read the measurements files from two microphones (two omnidirectional or one omnidirectional and one figure of eight) and to combine them in order to generate a first-order directional virtual microphone. This function returns two Matlab files containing the magnitude of the directivity response and the self-noise signal of the virtual microphone.

The function is called using a graphical user interface (see Fig. B.1) which requeries the user to select diferent options. The interface is organized on four pannels:

- Virtual Mic characteristics: This pannel contains the different options to generate a virtual first-order microphone such as the value of the parameter $b$ and the method used to generate the microphone.

- Measurement conditions: If the chosen method is using two omnidirectional microphones it is necessary to introduce the distance between the measured microphones. It is also required to introduce the angular difference between adjacent measurements ($2°$ has been used in this thesis).

- Graphical options: The function is capable of represent the results depending on the choices of the user i.e. cartesian coordinates measured directivity pattern, polar coordinates measured directivity pattern, mean directivity pattern. It is also possible to apply an angular correction to the generated directivity patterns only for representation purposes in order to compare them with theoretical patterns.

- Frequencies selected: The frequencies selected in this pannel will determine the frequency range for which the virtual generated microphone will be created.
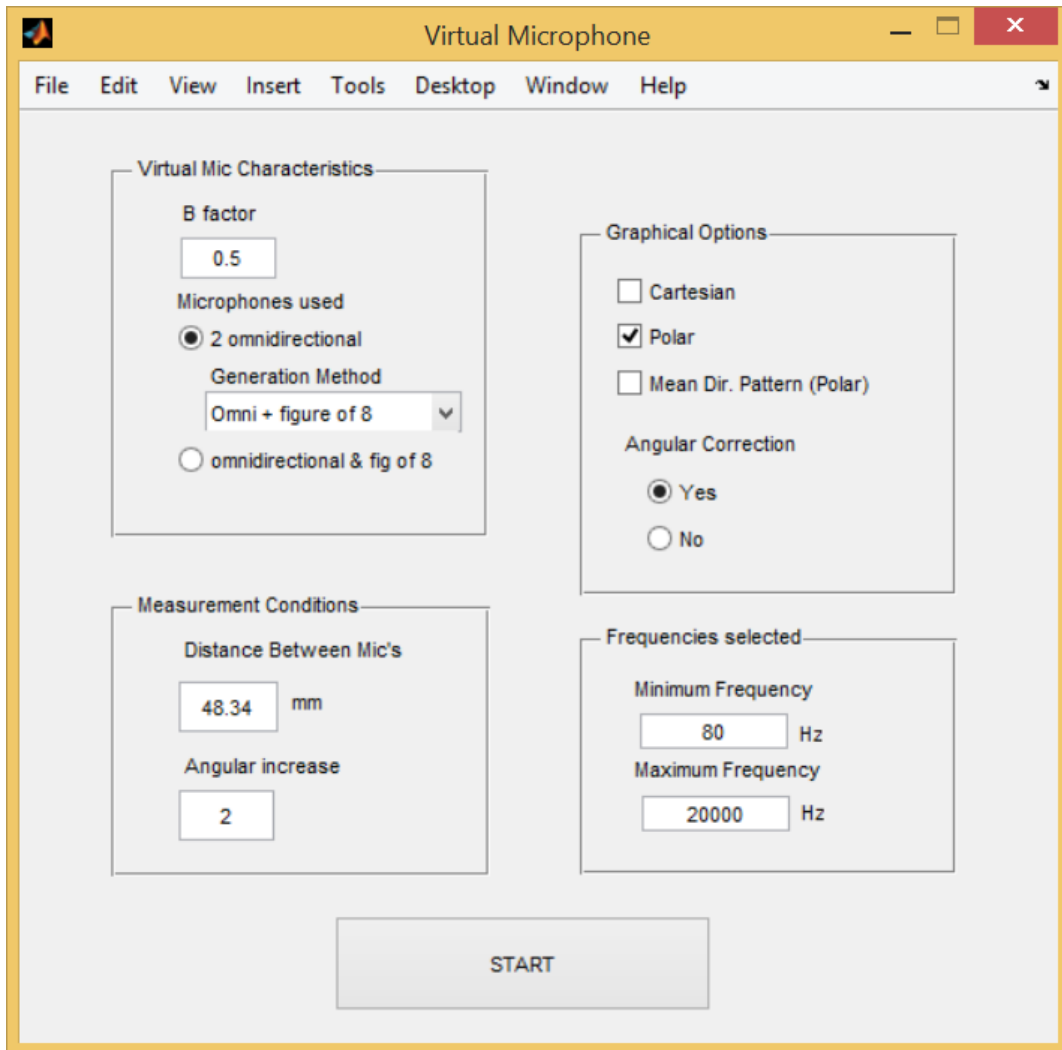
Figure B.1: Virtual Microphone function graphic user interface

Figure B.2 shows an example of the plots that this funtion can generate. In this
example the selcted pattern is a figure of 8.
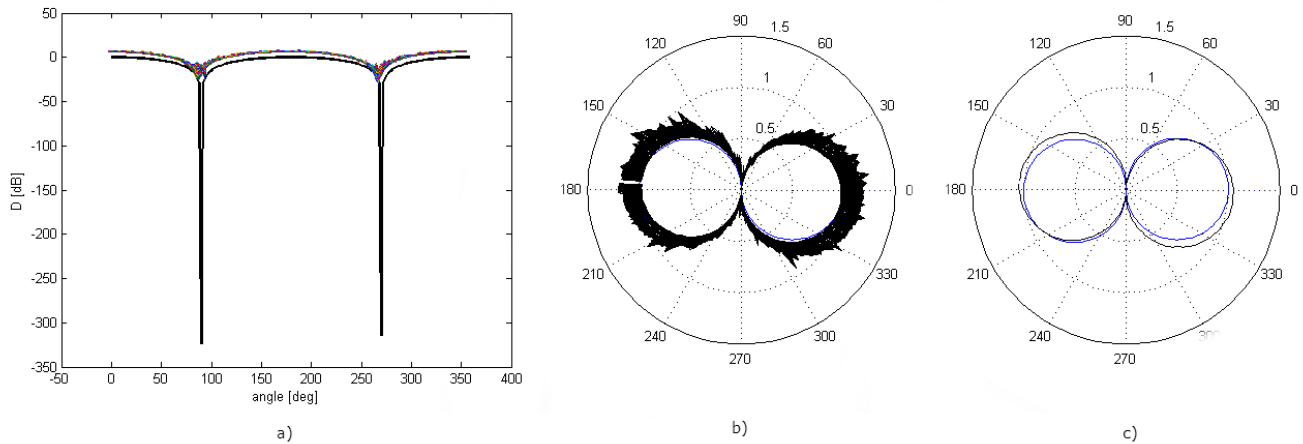
Figure B.2: Results generated by the Virtual Microphone function: a) Cartesian directivity pattern, b) Polar 2D directivity pattern, c) Polar 2D mean directivity pattern

## B.1.2  Performed operations

The acquisition system creates a file containing the impulsional response of each individual sensor in the set-up for every measurement. Firstly, it is necessary to import the WinMLS files into the Matlab environment. The format of the generated files is '.wmb' and they can be imported using the function LOADIMP.m [9]. This function returns the data, sampling frequency and format of the read file.

The first file imported is the microphones self noise recordings. This data will be lately used for computing the signal-to-noise ratio of the virtual microphone. The user is asked to select the folder in which the noise file is located. Once this signal is imported it is transformed to the frequency domain using the Fourier transform.

To import and process the impulse response of the two sensors acquiered in each measurement, the function loops over the incident angle values and the data of every next measurement is acquired and treated. The imported impulse response is zero padded and transformed into the frequency domain. Then the signals are combined following the method chosen by the user and the directivity data for a specified incident angle is created. This loop is repited from 0 degrees to 358 degrees in order to obtain directivity data for all the incident angles.

Afterwards, the created data of directivity magnitude and noise is stored into the output parameters.

The last step is to represent the directivity data according to the user's choice.

A diagram of the sequence of operations performed by this function is shown in Fig. B.3.
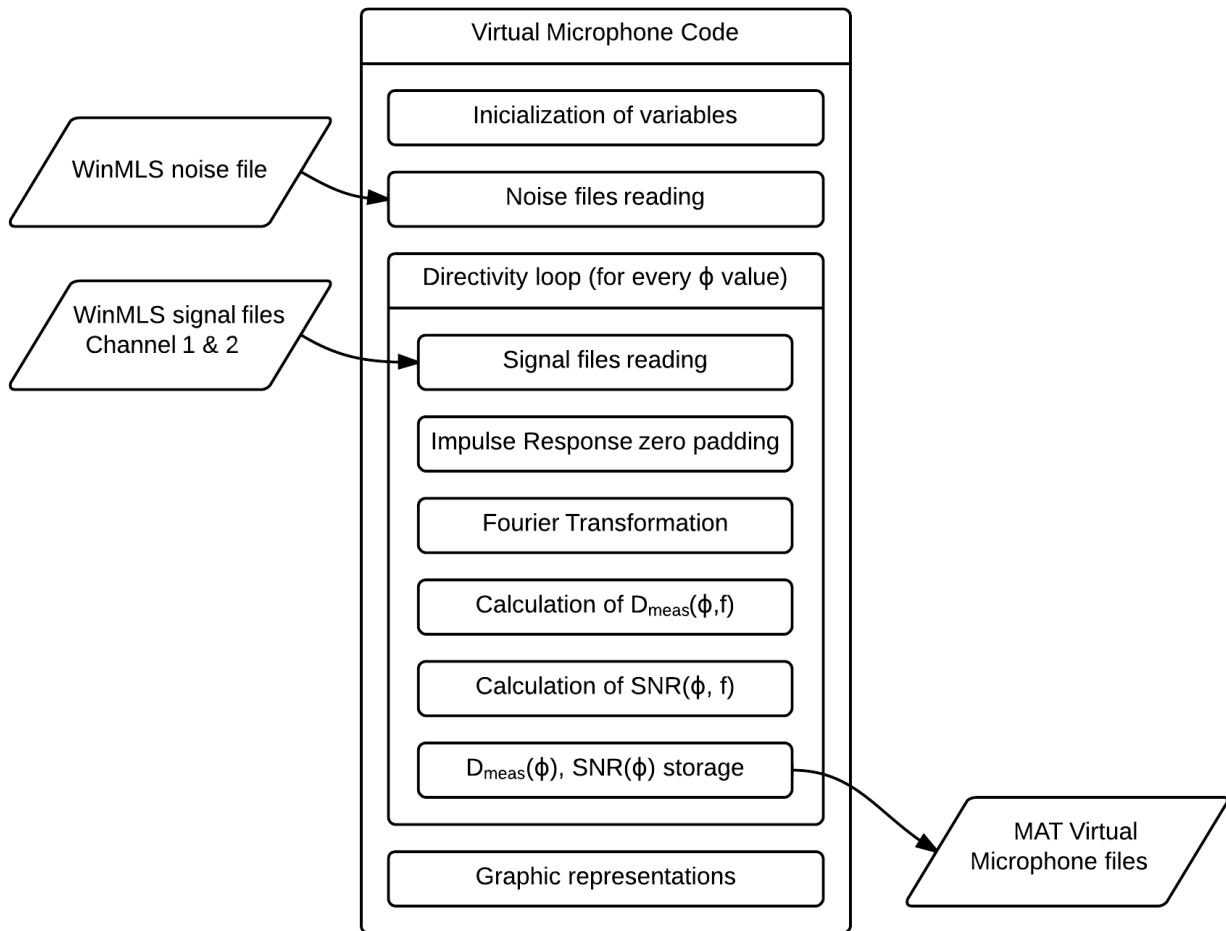
Figure B.3: Sequence of operations performed in the Virtual Microphone function

## B.1.3 MatLab code

```matlab
%%%%%%%%%%%%%%%%%%%%%%%%%%%%%%%%%%%%%%%%%%%%%%%%%%%%%%%%%%%%%%%%%%%%%%%%%%%%%%%
% Function Virtual Microphone: Creates a virtual first-order microphone %
% using the selected input data. %
% Input variables: %
%   - dirfac: directivity factor(1-b) (0=omnidirectional, 1=figure of 8)%
%   - Delta_theta: angular increase between measurements %
%   - method: generation method (2omni: DAS, back-to-back, omni8; omni+8%
%   - L: distance between microphones in milimeters %
%   - cart: cartesian pattern representation (1=on) %
%   - pol: polar pattern representation (1=on) %
%   - meandir: mean polar pattern representation (1=on) %
```

65

```matlab
12  %    - angcorr: angular correction (only for representations, 1=on)      %
13  %    - downfreq: minimum frequency of generation                         %
14  %    - upfreq: maximum frequency of generation                           %
15  % Output variables:                                                      %
16  %    - magnitude: generated directivity pattern                          %
17  %    - noise: SNR of the generated microphone                            %
18  % Note: It is recommended to use this function with the included         %
19  % GUI (guitest.m & guitest.fig)                                          %
20  %%%%%%%%%%%%%%%%%%%%%%%%%%%%%%%%%%%%%%%%%%%%%%%%%%%%%%%%%%%%%%%%%%%%%%%%%%%%
21
22  function [magnitude, noise] = virtual_mic(dirfac, Delta_theta, method,...
23      L, cart, pol, meandir, angcorr, downfreq, upfreq)
24
25  % Variables initialization
26  c=343.200;
27  L = L/1000;
28
29  % Set the names for the input files
30  dirname = uigetdir('./', 'Select the Folder for the Input Data ');
31
32
33  % Using an omnidirectional and figure of 8 microphone.
34  if method ==4
35      % The next two lines have to be modified depending on the test
36      % microphones used:
37      % - AKG cardioid capsule: remove 'Ch2' and 'Ch1'.
38      % - Soundfield microphone: include 'Ch3' and Ch4'.
39      % - AVS-Microflown: include 'Ch2' and Ch1'.
40
41      % Set the name of the noise files
42      filenameCh1N=[dirname '\IRN' num2str(0) 'Ch2.wmb'];
43      filenameCh2N=[dirname '\IRN' num2str(0) 'Ch1.wmb'];
44
45  % Combining the signal from two omnidirectional microphones
46  else
47      % Set the name of the noise files
48      filenameCh1N=[dirname '\IRN' num2str(0) 'Ch1.wmb'];
49      filenameCh2N=[dirname '\IRN' num2str(0) 'Ch2.wmb'];
50  end
51
52  % Sett the name of the files signal containing loudspeaker and room
53  % information
54  Ref=[dirname '\Ref.wmb'];
55
56
57  % Load background noise and reference
58  [N_Ch1,Fs_N_CH1]=LOADIMP(filenameCh1N);
59  [N_Ch2,Fs_N_CH2]=LOADIMP(filenameCh2N);
60  [Ref,Fs_Ref]=LOADIMP(Ref);
61
62  % Create the angular vector
63  Theta_vec=0:Delta_theta:360-Delta_theta;
```

```matlab
64
65 % Initializing the output vectors
66 samples = length(N_Ch1);
67 ABS_TF_dir=zeros(length(Theta_vec),samples);
68 ANG_TF_dir=zeros(length(Theta_vec),samples);
69 ABS_SNR_dir=zeros(length(Theta_vec),samples);
70
71 %Zero pad of the reference signal
72 Ref=Zero_Padding__(Ref);
73
74 %Calculate transfer functions (Ref & Noise)
75 TF_REF=fft(Ref);
76 TFN_Ch1=fft(N_Ch1);
77 TFN_Ch2=fft(N_Ch2);
78
79 % Create the directivity information for all the angles
80 for n=1:length(Theta_vec)
81     % Using an omnidirectional and figure of 8 microphone.
82     if method == 4
83
84         % The next two lines have to be modified depending on the test
85         % microphones used:
86         % - AKG cardioid capsule: remove 'Ch2' and 'Ch1'.
87         % - Soundfield microphone: include 'Ch3' and Ch4'.
88         % - AVS-Microflown: include 'Ch2' and Ch1'.
89
90         % Set the name of the signal files at every angle
91         filenameCh1=[dirname '\IR' num2str(Theta_vec(n)) 'Ch2.wmb'];
92         filenameCh2=[dirname '\IR' num2str(Theta_vec(n)) 'Ch1.wmb'];
93     % Combining the signal from two omnidirectional microphones
94     else
95         % Set the name of the signal files at every angle
96         filenameCh1=[dirname '\IR' num2str(Theta_vec(n)) 'Ch1.wmb'];
97         filenameCh2=[dirname '\IR' num2str(Theta_vec(n)) 'Ch2.wmb'];
98     end
99
100     %Import data
101     [IR_Ch1,Fs_IR_CH1]=LOADIMP(filenameCh1);
102     [IR_Ch2,Fs_IR_CH2]=LOADIMP(filenameCh2);
103
104     %Zero padding
105     IR_Ch1=Zero_Padding__(IR_Ch1);
106     IR_Ch2=Zero_Padding__(IR_Ch2);
107
108     %Calculate transfer function
109     TF_Ch1=fft(IR_Ch1);
110     TF_Ch2=fft(IR_Ch2);
111
112     %Calculate frequency axes
113     Freq=0:Fs_IR_CH1/length(IR_Ch1):Fs_IR_CH1/length(IR_Ch1)* ...
114         (length(IR_Ch1)-1);
115
```

67

```matlab
116     %Consider only the range from downfreq to upfreq
117     Ind=find(downfreq <= Freq & upfreq>=Freq);
118
119     %Choose directivity factor
120     b = dirfac;
121     kvec=2*pi*Freq'/c;
122
123
124         % CREATE THE MICROPHONE
125     if method == 1
126         % Method 1: Omni +  figure of 8
127         TF_dir=(1-b)*0.5*(TF_Ch2+TF_Ch1)+ ...
128             b./(1i*kvec*L).*(TF_Ch2-TF_Ch1);
129         TFN_dir=(1-b)*0.5*(TFN_Ch2+TFN_Ch1)+ ...
130             b./(1i*kvec*L).*(TFN_Ch2-TFN_Ch1);
131
132         elseif method == 2
133         % Method 2: Back-to-Back Cardioid
134         bprim = 2*b - 1;
135         TF_dir = ((TF_Ch2 - TF_Ch1.*exp(1i*kvec*L)) - ...
136             bprim*(TF_Ch1 -  TF_Ch2.*exp(1i*kvec*L)))./(2*1i*kvec*L);
137         TFN_dir = ((TFN_Ch2 - TFN_Ch1.*exp(1i*kvec*L)) - ...
138             bprim*(TFN_Ch1  - TFN_Ch2.*exp(1i*kvec*L)))./(2*1i*kvec*L);
139
140         elseif method == 3
141         % Methord 3: Delay and sum
142         TF_dir = (TF_Ch1 - ...
143             TF_Ch2 .* exp((1i*kvec*L*(1-b))/(1-(1-b))))./(2*1i*kvec*L);
144         TFN_dir = (TFN_Ch1 - ...
145             TFN_Ch2 .* exp((1i*kvec*L*(1-b))/(1-(1-b))))./(2*1i*kvec*L);
146         elseif method == 4
147         TF_dir=(b)*(TF_Ch1)+(1-b).*(TF_Ch2);
148         TFN_dir=(b)*(TFN_Ch1)+(1-b).*(TFN_Ch2);
149     end
150
151     % Remove the influence of the loudspeaker and the room
152     TF_dir=TF_dir./abs(TF_REF);
153     TFN_dir=TFN_dir./abs(TF_REF);
154
155     % Compute SNR
156     SNR_dir=10*log10((abs(TF_dir).^2)./((abs(TFN_dir)).^2)-1);
157
158     %Save in the matrix
159
160     ABS_TF_dir(n,:)=abs(TF_dir);
161     ANG_TF_dir(n,:)=angle(TF_dir);
162     ABS_SNR_dir(n,:)=SNR_dir;
163
164     clear IR_Ch1 IR_Ch2
165 end
166
167 fclose('all');
```

68

```matlab
168
169 % OUTPUTS
170 magnitude = ABS_TF_dir(:,:);
171 noise = ABS_SNR_dir(:,:);
172
173 % FROM NOW, GRAPHICAL TOOLS
174
175 % Create the ideal pattern
176 D = (1-b)+b*cos((Theta_vec)*pi/180);
177
178 % Compute the mean measured pattern
179 ABS_TF_mean = mean(ABS_TF_dir(:,Ind)');
180
181 % Find the angle of maximum sensitivity
182 compmax = find(ABS_TF_mean == max(ABS_TF_mean),1);
183
184 % Create the angular vectors for the representations
185 thetapol = linspace(0,2*pi,360/Delta_theta);
186 if thetapol(compmax)>pi
187     newthetacart = (-thetapol(compmax)*360/(2*pi)- ...
188         180:Delta_theta:360-thetapol(compmax)*360/(2*pi)-Delta_theta-180);
189 elseif thetapol(compmax)<pi
190     newthetacart = (-thetapol(compmax)*360/(2*pi):Delta_theta:360- ...
191         thetapol(compmax)*360/(2*pi)-Delta_theta);
192 end
193 theta=[0:Delta_theta:360-Delta_theta];
194 newtheta = [-thetapol(compmax):2*pi/(360/Delta_theta):2*pi-...
195     thetapol(compmax)-2*pi/(360/Delta_theta) ];
196
197 % Cartesian representation
198 if cart == 1
199     ABS_TF_1000=ABS_TF_dir(1,2974)*ones(360/Delta_theta,samples);
200     D=(1-b)+b*cos((theta)*pi/180);
201     figure
202     plot(theta,20*log10(D),'k','LineWidth',2);
203     hold on
204     if angcorr == 0
205         plot(theta,20*log10(ABS_TF_dir(:,Ind))' ...
206             -20*log10(ABS_TF_1000(:,Ind))');
207     elseif angcorr == 1
208         plot(newthetacart+360,20*log10(ABS_TF_dir(:,Ind))' ...
209             -20*log10(ABS_TF_1000(:,Ind))');
210     end
211     xlabel ('angle [deg]')
212     ylabel ('D [dB]')
213 end
214
215
216 % Polar representation of the measured pattern
217 ax = max(max(ABS_TF_dir(:,Ind)));
218 if pol == 1
219     figure
```

```matlab
220      if ax>1
221          polar(0,ax)
222          hold on;
223      end
224      polar(thetapol,abs(D));
225      hold on;
226      for k=1:length(ABS_TF_dir(:,Ind))
227          if angcorr == 0
228              polar(thetapol,(ABS_TF_dir(:,Ind(k)))','k');
229          elseif angcorr == 1
230              polar(newtheta,(ABS_TF_dir(:,Ind(k)))','k');
231          end
232      end
233  end
234
235  % Polar representation of the mean of the measured pattern
236  if meandir == 1
237      figure
238      if ax>1
239          polar(0,ax)
240      hold on;
241      end
242      polar(thetapol, abs(D));
243      hold on;
244      if angcorr == 1
245          polar(newtheta, ABS_TF_mean,'k');
246      elseif angcorr == 0
247          polar(thetapol, ABS_TF_mean,'k');
248      end
249  end
```

## B.2  Analysis function

### B.2.1  Description

This function computes and plots the Frequency Response Function, the Directivity Error and the signal-to-noise ratio of the virtual microphone.

The user can select the different options to perform the analysis of the microphones: the nature of the input files (WinMLS files or MAT files), the angular difference between measurements, the minimum and maximum frequency of analysis, the application of angular correction, graphic options and the value of the parameter $b$ of the directivity pattern.

The output parameters of the function are three vectors containing the Frequency Response Function, the Directivity Error and the signal-to-noise ratio of the analyzed microphone. The function also generates image files (.png) of the output parameters.

## B.2.2 Performed operations

After calling the function the user is asked to specify the folder in which the input data is located. If the selected data comes from a WinMLS file, the measurement data is treated in order to obtain the Fourier transform of the impulsional response. Otherwise, if the selected data comes from a MAT file it is not necessary to perform these operations.

The next step is to generate a vector with the theoretical directivity pattern selected. Once this vector is created, the Frequency Response Function is calculated by comparing the response of the microphone at the main axis with the theoretical response as in Equations 4.1 to 4.6. After that, the measured pattern is scaled in order to minimize the Directivity Error. The Directivity Error is computed comparing the difference of the adjusted measured pattern with the theoretical pattern as in Equations 4.7. Finally, using the microphone's self-noise spectrum and the FRF on the main axis of the microphone or array the signal-to-noise ratio is computated.

## B.2.3 Matlab code

```matlab
%%%%%%%%%%%%%%%%%%%%%%%%%%%%%%%%%%%%%%%%%%%%%%%%%%%%%%%%%%%%%%%%%%%%%%%%%%%
% Function Mic Analysis: Computes the performance of a first-order mic  %
% in terms of FRF, Directivity error and SNR.                          %
% Input variables:                                                     %
%   - matfile: selects if input data is WinMLS data(0) or .mat files(1) %
%   - Delta_theta: angular increase between measurements               %
%   - downfreq: minimum frequency of generation                        %
%   - upfreq: maximum frequency of generation                          %
%   - angcorr: angular correction (only for representations, 1=on)     %
%   - plotpat: representation of the polar pattern (1=on / 0=off)      %
%   - b: directivity factor of the ideal pattern (0=omni, 1=fig8)      %
% Output variables:                                                    %
%   - freqvec: frequencies vector                                      %
%   - FRF: vector containing FRF function of the mic                   %
%   - DirError: vector containing the directivity error of the mic     %
%   - SNR: vector containing the SNR data of the mic                   %
% Note: It is recommended to use this function with .mat files obtained %
% from the function virtual_mic.m (guitest.m & guitest.fig)            %
%%%%%%%%%%%%%%%%%%%%%%%%%%%%%%%%%%%%%%%%%%%%%%%%%%%%%%%%%%%%%%%%%%%%%%%%%%%

function [freqvec, FRF, DirError, SNR] = mic_analysis(matfile, ...
    Delta_theta, downfreq, upfreq, angcorr, plotpat, b)

% Create angular vector
Theta_vec=0:Delta_theta:360-Delta_theta;

% Loading the loudspeaker and room data
dirname = uigetdir('./', 'Select the Folder for the Input Data ');
Ref=[dirname '\Ref.wmb'];
[Ref,Fs_Ref]=LOADIMP(Ref);
Ref=Zero_Padding__(Ref);
```

```matlab
32  TF_REF=fft(Ref);
33
34  % Initializing variables
35  samples = length(Ref);
36  ABS_TF_dir=zeros(length(Theta_vec),samples);
37
38  if matfile == 0 % Read WinMLS files directly (for real microphones)
39      [filenameN, pathnameN] = uigetfile;
40      [IR_N,Fs_IR_N]=LOADIMP([pathnameN filenameN]);
41      IR_N=Zero_Padding__(IR_N);
42      TF_N=fft(IR_N);
43      for n=1:length(Theta_vec) % Create the data vectors
44          filenameCh1=[dirname '\IR' num2str(Theta_vec(n))  '.wmb'];
45          [IR_Ch1,Fs_IR_CH1]=LOADIMP(filenameCh1); % Load data
46          IR_Ch1=Zero_Padding__(IR_Ch1); % Zero pad the IR
47          TF_Ch1=fft(IR_Ch1); % TF of the IR
48          Freq=0:Fs_IR_CH1/length(IR_Ch1):... % Creating freqs vector
49              Fs_IR_CH1/length(IR_Ch1)*(length(IR_Ch1)-1);
50          TF_Ch1 = TF_Ch1./abs(TF_REF); % Removing room and speaker data
51          ABS_TF_dir(n,:)=abs(TF_Ch1); % Saving data variables
52          clear IR_Ch1 IR_Ch2
53      end
54  else % Read .mat files (for virtual mics created with virtual_mic.m)
55          [filename,pathname] = uigetfile;
56          load([pathname filename],'noisevar');
57          TF_N = noisevar;
58          [filename,pathname] = uigetfile(pathname);
59          load([pathname filename],'magnitudevar');
60          ABS_TF_dir = magnitudevar;
61          Freq=0:Fs_Ref/length(Ref):Fs_Ref/length(Ref)*(length(Ref)-1);
62  end
63
64  % Consider range from downfreq to upfreq
65  Ind=find(downfreq <= Freq & upfreq>=Freq);
66
67  fclose('all');
68
69  % Find the angle of maximum magnitude
70  IndLowFreq=find(400 <= Freq & 900>=Freq);
71  ABS_TF_mean_lowfreq = mean(ABS_TF_dir(:,IndLowFreq)');
72  compmax = find(ABS_TF_mean_lowfreq == max(ABS_TF_mean_lowfreq),1);
73
74  % Angular vector
75  thetapol = linspace(0,2*pi-Delta_theta*pi/180,360/Delta_theta);
76
77  % Ideal pattern
78  D = abs((1-b)+b*cos((Theta_vec)*pi/180));
79
80  % Angular correction of the measured pattern
81  D_meas = [ABS_TF_dir(compmax:180,Ind) ; ABS_TF_dir(1:compmax-1, Ind)];
82
83  % Computation of A(w) and scaling measured pattern
```

```matlab
84  for k=1:length(ABS_TF_dir(:,Ind))
85          sumcorrDDmeas(:,k) = abs(sum(D_meas(:,k)'.*D));
86  end
87  sumcorrmeas = abs(sum(D_meas(:,:).*D_meas(:,:)));
88  A = sumcorrDDmeas ./ sumcorrmeas;
89  for k=1:length(ABS_TF_dir(:,Ind))
90      D_meas_comp(:,k) = D_meas(:,k)'.*A(k);
91  end
92
93  % Plot and save scaled pattern
94  if plotpat == 1
95      fig1 = figure('units','normalized','outerposition',[0 0 1 1]);
96      polar(0,1);
97      hold on;
98      polar(thetapol, abs(D));
99      for k=1:length(ABS_TF_dir(:,Ind))
100         if angcorr == 1
101             polar(thetapol, D_meas_comp(:,k)','k');
102         elseif angcorr == 0
103             polar(thetapol, D_meas_comp,'k');
104         end
105     end
106     saveas(fig1,'scaledpattern','fig');
107     set(gcf,'PaperUnits','centimeters','PaperPosition',[0 0 30 15])
108     print('-dpng', 'scaledpattern.png', '-r700');
109 end
110
111
112 % Plot and save Freq. Response function
113 fig2 = figure('units','normalized','outerposition',[0 0 1 1]);
114 freqresp = 10*log(1./A);
115 semilogx(Freq(Ind), freqresp, 'LineWidth',2);
116 Dmatrix = repmat(D,length(Ind),1);
117 set(gca,'XTick',[80 100 500 1000 2000 4000 10000 20000],'FontSize', 14)
118 axis([downfreq upfreq min(freqresp)-0.05*abs(min(freqresp)) ...
119     max(freqresp)+0.05*abs(max(freqresp))])
120 title('Frequency Response Function' ,'FontSize', 20);
121 xlabel('Frequency (Hz)','FontSize', 15);
122 ylabel('$$10 \log \frac{1}{A(\omega)} (dB)$$',...
123     'Interpreter','Latex','FontSize', 14)
124 grid on;
125 saveas(fig2,[pathname 'freqresponse'],'fig');
126 set(gcf,'PaperUnits','centimeters','PaperPosition',[0 0 30 15])
127 print('-dpng',[pathname 'freqresponse.png'], '-r700');
128
129 % Compute Directivity Error
130 SSres = sum(D_meas_comp - Dmatrix').^2;
131 error = SSres;
132
133 % Plot and save Directivity Error
134 % Linear scale (error)
135 fig4 = figure('units','normalized','outerposition',[0 0 1 1]);
```

73

```matlab
136  semilogx(Freq(Ind), error,'LineWidth',2);
137  set(gca,'XTick',[80 100 500 1000 2000 4000 10000 20000],'FontSize',14)
138  axis([downfreq upfreq 0 max(error)+0.05*max(error)])
139  title('Directivity Error (Linear scale)','FontSize', 14);
140  xlabel('Frequency (Hz)');
141  ylabel('$$\xi(\omega)$$','Interpreter','Latex','FontSize', 14)
142  grid on;
143  saveas(fig4,[pathname 'errorlineal'],'fig');
144  set(gcf,'PaperUnits','centimeters','PaperPosition',[0 0 30 15])
145  print('-dpng',[pathname 'errorlineal.png'], '-r700');
146
147  % Logarithmic scale (error)
148  fig5 = figure('units','normalized','outerposition',[0 0 1 1]);
149  loglog(Freq(Ind), error,'LineWidth',2);
150  set(gca,'XTick',[80 100 500 1000 2000 4000 10000 20000],'FontSize', 14)
151  set(gca,'YTick',[10^-6 10^-5 10^-4 10^-3 10^-2 10^-1 10^0 10^1 10^2], ...
152      'FontSize', 14)
153  axis([downfreq upfreq 0 max(error)+0.05*max(error)])
154  title('Directivity Error (Logarithmic scale)','FontSize', 14);
155  xlabel('Frequency (Hz)','FontSize', 14);
156  ylabel('$$\xi(\omega)$$','Interpreter','Latex','FontSize', 14)
157  grid on;
158  saveas(fig5,[pathname 'errorlog'],'fig');
159  set(fig5,'PaperUnits','centimeters','PaperPosition',[0 0 30 15])
160  print('-dpng',[pathname 'errorlog.png'], '-r700');
161
162  % Compute SNR
163  Noise = [TF_N(compmax:180,Ind) ; TF_N(1:compmax-1, Ind)];
164  Noise1 = abs(Noise(1,:));
165  Noisesmooth = smooth(Noise1,50); % Smoothing the SNR results (50 samples)
166
167  % Plot the SNR
168  fig = figure('units','normalized','outerposition',[0 0 1 1]);
169  semilogx(Freq(Ind),Noisesmooth,'LineWidth',2);
170  set(gca,'XTick',[80 100 500 1000 2000 4000 10000 20000],'FontSize', 14);
171  set(gca,'YTick',[10 20 30 40 50 60 70 80 90 100 110 120 130 140 150], ...
172      'FontSize', 14);
173  title('Signal-to-Noise Ratio','FontSize', 14);
174  xlabel('Frequency (Hz)','FontSize', 14);
175  ylabel('$$20 \times \log \frac{S}{N} (dB)$$','Interpreter','Latex', ...
176      'FontSize', 14);
177  axis([downfreq upfreq 0 max(Noise(1,:))+10]);
178  grid on;
179  saveas(fig,[pathname '\SNR'],'fig');
180  set(fig,'PaperUnits','centimeters','PaperPosition',[0 0 30 15])
181  print('-dpng',[pathname '\snr.png'], '-r700');
182
183  % Set output variables
184  FRF = freqresp;
185  DirError = error;
186  freqvec = Freq(Ind);
187  SNR = Noisesmooth';
```

74

```matlab
188
189  % Save output variables
190  save([pathname 'results'], 'FRF','DirError','SNR');
```